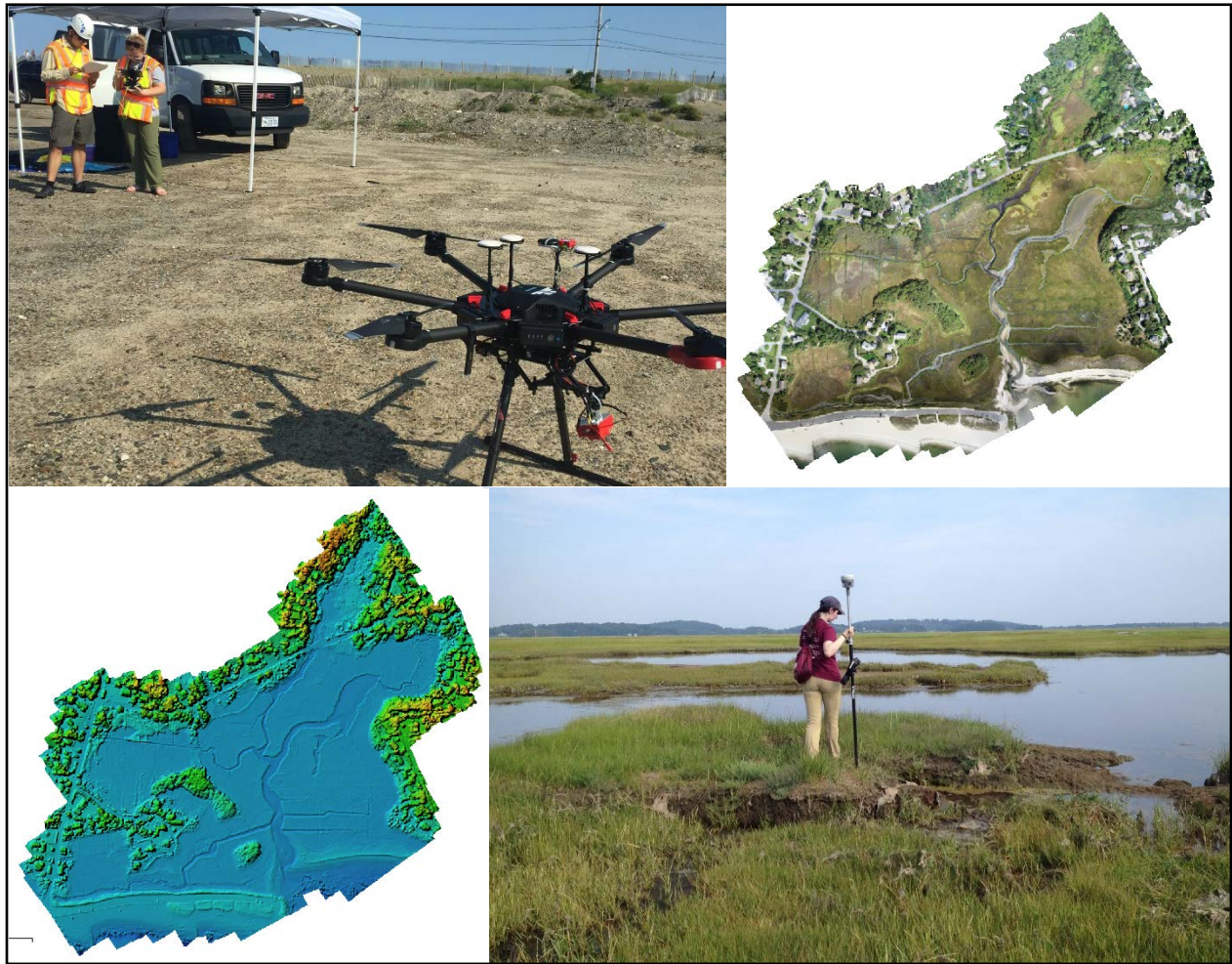


Developing Methods for Remote Sensing of Salt Marsh Condition using Unoccupied Aerial Systems (UAS)

July 26, 2021

Scott Jackson, Amanda Davis, Kate Fickas, Ryan Wicks, Joshua Ward
and Charles Schweik

University of Massachusetts Amherst



This is the final report for EPA FY 2017-2018 Wetlands Program Development
Grant CD 00A00312-3

Introduction

The Conservation Assessment and Prioritization System (CAPS) is a computer model and sophisticated approach to assessing the ecological integrity of ecosystems. It is being used as a Level 1 assessment methodology as part of a comprehensive wetlands assessment and monitoring program for Massachusetts. When credible models of ecological integrity can be developed we use them to get a comprehensive assessment of all Massachusetts wetlands and use it to guide field-based assessments (rapid or intensive) and policy/management to maintain or improve wetland condition.

For the past several years we have been using data collected in the field to compare the Indices of Ecological Integrity (IEI) calculated by CAPS with biological field data collected in streams, forested wetlands, salt marshes, and, more recently, shrub swamps. From these field data we have been able to calculate robust Indices of Biological Integrity (IBIs) that correspond to IEI gradients for streams and forested wetland, but not salt marshes. Salt marshes are probably the most threatened wetland type in Massachusetts and are particularly vulnerable to the effects of climate change, especially sea level rise.

We have several possible explanations for why we have not yet been able to correlate CAPS IEI scores with field indices of salt marsh condition.

1. Biological data collection has focused on the wrong taxa (plants and invertebrates). Perhaps other taxa (e.g. birds, fish) would be better indicators of salt marsh condition.
2. Methods for sampling invertebrates and vegetation in salt marshes were not sufficient/appropriate.
3. Given the low diversity of salt marsh plants and the tendency for large areas of salt marsh to be dominated by 2-3 species, perhaps species composition is the wrong metric for assessing vegetation. An alternative might be an assessment of plant health and productivity.
4. Given the low diversity of salt marsh plants, perhaps it would be more appropriate to use physical indicators (creek widening, creek bank instability, peat density, inappropriate high marsh flooding) to assess salt marsh condition.
5. The CAPS IEI model for salt marshes lacks metrics for important salt marsh stressors related to sediment dynamics, effects of increased nutrient loading on peat accretion, changes in marsh elevation relative to sea level rise, crab herbivory, and crab burrowing effects on peat density and stability.

Any, all, or various combinations of these factors may be affecting our ability to model ecological integrity or assess condition in the field for salt marshes. This project investigates alternative ways of assessing salt marshes focusing on physical indicators of marsh condition and plant stress/productivity (addressing explanations 3-5 above).

Field work in salt marshes is difficult because tide cycles affect our ability to access interior portions of marshes and to see/evaluate marsh characteristics due to ever changing water levels. Remote sensing (satellite imagery; aerial photographs) offers some potential for assessing salt marsh characteristics. However, these data may not be available at stages in the tide cycle when specific characteristics need

to be assessed, such as high tide for assessing high marsh flooding or low tide for assessing creek bank stability.

In 2018, we initiated a project to investigate the use of unoccupied aerial systems (UAS) to collect data when timing is critical and test the potential of using various sensors to assess vegetation health/stress and physical characteristics of salt marshes. The goal is to use UAS technology as part of a nested approach to remote sensing (also including satellite data and aerial photographs) to assess the physical and perhaps biological (e.g. plant stress) condition of salt marshes. Ultimately, we hope to develop more effective CAPS metrics for assessing IEI of salt marshes by investigating, developing and using UAS-based remote sensing techniques, or using finer scale UAS data to help inform satellite image (e.g., Landsat) analyses.

This first phase of the project focused on characterizing land cover and identifying threats and vulnerabilities in salt marshes by UAS flights to capture multispectral and multi-temporal data collected at different tidal stages and across field seasons to assess the condition of salt marshes. A related goal was to investigate, develop and refine UAS-related data collection and image analysis methodologies that can be replicated to assess salt marshes in Massachusetts and throughout New England.

This report summarizes our approach and progress characterizing land cover and identifying threats and vulnerabilities in salt marshes during 2018 through 2020. We frequently refer to our approved Quality Assurance Project Plan (QAPP) which contains more detailed information about our protocols. Here, we discuss our sites, methods for data collection and data analysis, and our results. We also comment on challenges, limitations, and our next steps for this ongoing project.

ACKNOWLEDGEMENTS

We appreciate the towns, landowners, and land conservation organizations who have supported this project by providing permits, access to field sites, facilities, and personnel. It has been a pleasure to work with The Trustees of Reservations, the Massachusetts Audubon Society, Harwich Conservation Trust, Chatham Conservation Commission, MA Coastal Zone Management (CZM), the Town of Scituate, the Scituate Country Club, Massachusetts Department of Conservation and Recreation (DCR), the Marine Biological Laboratory, and the Woods Hole Research Center. We acknowledge and thank the following people who materially contributed to this project: Marc Carullo, Helena Koszewski, Daniel Myers, Emily Lozier, Brett Barnard, David Price and Devin Clark. Additional support for this work was provided by the UMass Center for Agriculture, Food, and the Environment, in the form of Summer Scholarships for students who worked on the project.

Methods

DEVELOP AND SUBMIT QAPPS

A Quality Assurance Project Plan (QAPP) was developed by project personnel and collaborators for every component of this research project. The QAPP contains Standard Operating Procedures (SOPs), safety considerations, information about sites and collaborators, data quality procedures and objectives, and details about equipment. The QAPP includes the following appendices.

- Appendix A - Remote Sensing via Unoccupied Aerial Systems (UAS)
- Appendix B - Analysis of UAS Imagery to Characterize Tidal Hydrology, Identify Areas of Salt Marsh Erosion and Create Base Maps for Field Data Collection
- Appendix C - Ground-Based Field Data Collection
- Appendix D - Remote Sensing Image Classification Model
- Appendix E - Salt Marsh Classification

Work commenced once the QAPP was approved by the EPA. Changes to the QAPP were made in response to unanticipated challenges in the field and with equipment. When this occurred, deviations from the QAPP were recorded and the QAPP was revised and resubmitted for approval.

PERMITTING & PERMISSIONS

Prior to the field season, permissions were obtained or renewed from the landowner or managing agency for each field site. Prior to each UAS flight, air space permissions were obtained from air traffic controllers from any proximate airports (i.e. airports that are within 5 miles) and others according to protocol in Appendix A.

STUDY SITES

We worked collaboratively with partners to collect data from nine salt marshes in Massachusetts from 2018 – 2020 (Figure 1). Sites along the North Shore of Massachusetts were Old Town Hill (Newbury) and Essex Bay (Essex). Sites along the South Shore were Peggotty Beach (Scituate), North River (Scituate), and South River (Marshfield). Sites on Cape Cod were Barnstable Great Marsh (Barnstable), Red River (Harwich and Chatham), and Wellfleet Bay Wildlife Sanctuary (Wellfleet). One site, Horseneck Beach (Westport), was on the coast of Buzzard's Bay. Each site had its own mix of hydrology, stressors, anthropogenic activities, and history of natural events. Below is a brief description for each of the nine salt marsh sites.

After we established an initial study area footprint for each site, it was decided to reduce the footprint size for several of the sites (to approximately 100 acres) to reduce the time required to fly the designated study areas. Reducing the time needed to acquire UAS imagery help ensure that tide conditions did not significantly change between the beginning and end of each flight.



Figure 1. Yellow pins identify the nine salt marsh sites that we assessed from 2018-2020 in Massachusetts.

Old Town Hill

The Old Town Hill site (Figure 2) is located a few miles west of Plum Island and was selected because of specific interest expressed by The Trustees of Reservations (TTOR) which owns the land. TTOR has committed significant resources to studying a portion of the site, including developing a Sea Level Affecting Marshes Model (SLAMM) of land cover change over the next 50 years, which will complement the data that we collect. In 2020, TTOR began a salt marsh ditch remediation effort with an innovative nature-based method that was piloted at the U.S. Fish and Wildlife Service's Parker River National Wildlife Refuge. Walking trails are found throughout this site and it is a popular place for recreation and bird watching. Historically, this marsh was used to produce and harvest salt hay.

We installed 16 Ground Control Points (GCPs) (blue markers) at Old Town Hill that help us accurately georeference the imagery we collect so that they can be “stacked” and analyzed as a longitudinal dataset using geographic information systems (GIS) and other remote sensing analytic techniques. The full flight footprint covered 206 acres (outlined in blue) and had a perimeter of 3.8 miles. The reduced flight footprint covered 100 acres (outlined in bright pink) and had a perimeter of 2.26 miles.

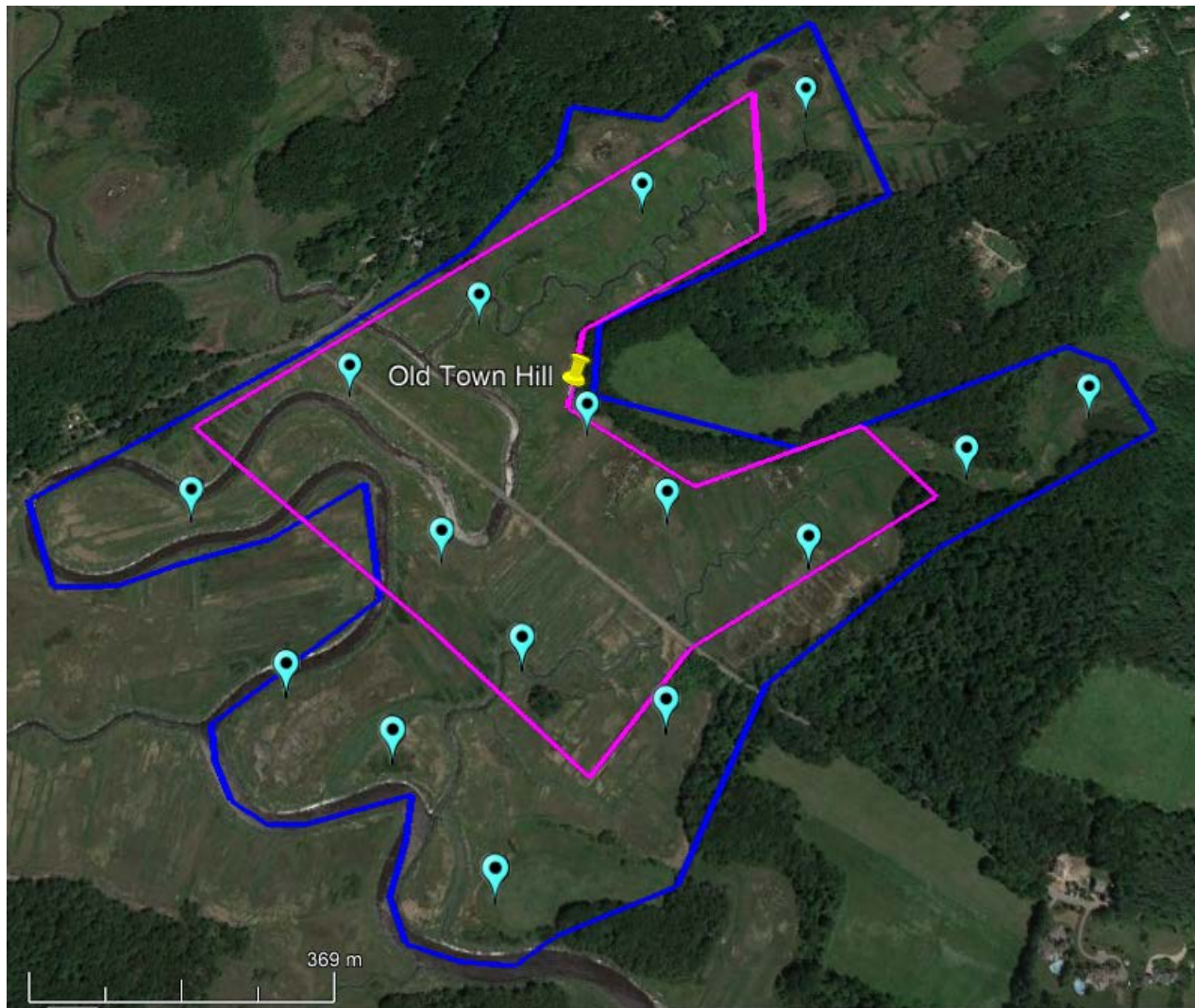


Figure 2. Old Town Hill (Newbury, MA) - Partnered with The Trustees of Reservations

Essex Bay

The Essex Bay site (Figure 3) contains Dean's Island and is located behind the Cape Ann Golf Course. It was selected because of specific interest expressed by The Trustees of Reservations which owns the land, and because it is a sentinel site being studied by MA Coastal Zone Management. During the winter of 2018, extreme cold, winds, and storm surge created notable sediment deposition events throughout the Great Marsh Estuary, which includes Essex Bay. A report about this event in Essex Bay has been published by Moore et al. 2019 from the University of New Hampshire.

We installed 14 GCPs (blue markers) throughout the Essex Bay study site. The full flight footprint covered 215 acres (outlined in blue) and had a perimeter of 2.3 miles. The reduced flight footprint covered 100 acres (outlined in bright pink) and had a perimeter of 1.53 miles.

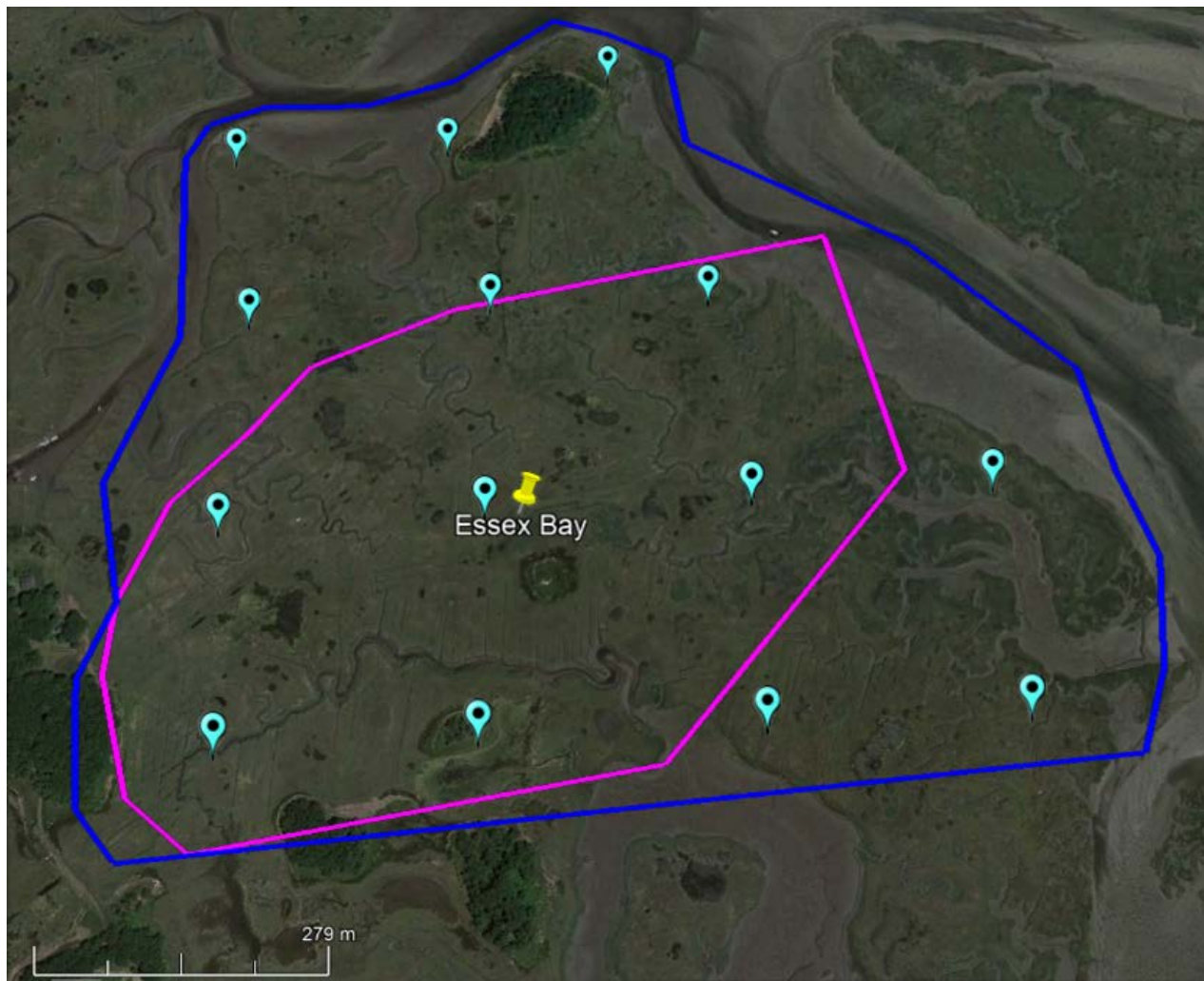


Figure 3. Essex Bay (Essex, MA) - Partnered with The Trustees of Reservations and MA Coastal Zone Management

Peggotty Beach

This site at Peggotty Beach (Figure 4) is located in the town of Scituate. It was selected because an intensive study being conducted by a team of geologists from UMass Amherst will provide us with complementary data on sediment dynamics in this marsh. Nor'easters during the winter of 2018 drastically altered the beach and adjacent salt marsh morphology. This site presented an opportunity to study differences in spectral signatures associated with a rapidly changing salt marsh.

We installed 7 GCPs (blue markers) throughout the Peggotty Beach marsh. The full flight footprint covered 104 acres (outlined in bright pink) and had a perimeter of 1.88 miles. A reduced flight footprint was not needed for this site.

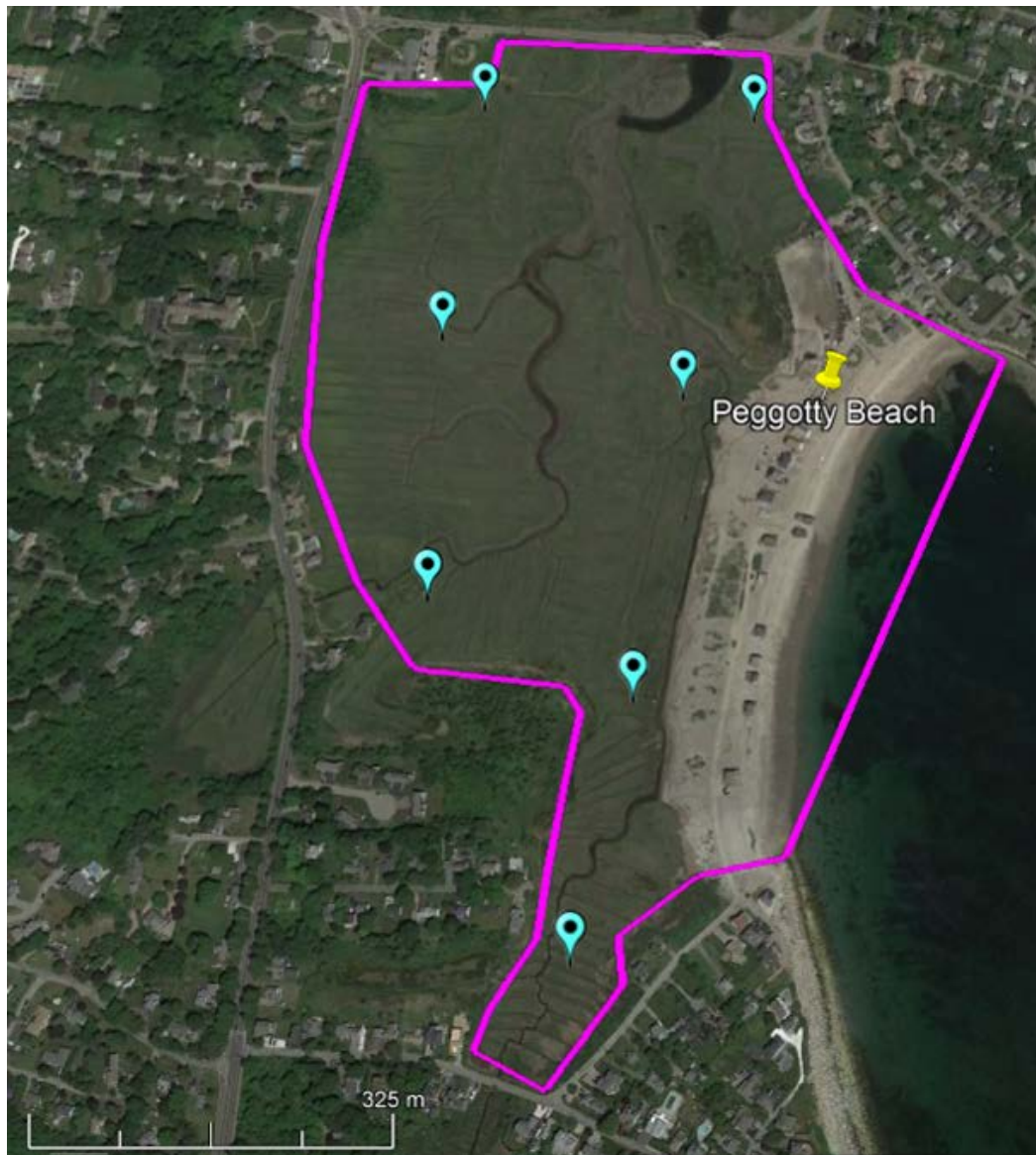


Figure 4. Peggotty Beach (Scituate, MA) - Partnered with UMass Amherst Geosciences Department

North River

The North River marsh site (Figure 5) is located at the mouth of the North River in the town of Scituate and contains portions of marsh owned by the Scituate Country Club. The beach area is overseen by the Massachusetts Audubon Society. This site was selected because 1) an intensive study being conducted by a team of geologists from UMass Amherst will provide complementary data on sediment dynamics, and 2) the opportunity to capture changes in beach morphology that is important to nesting birds.

We installed 9 GCPs (blue markers) throughout the North River inlet. The full flight footprint covered 163 acres (outlined in blue) and had a perimeter of 2.43 miles. A reduced flight footprint (outlined in bright pink) covered 90 acres and had a perimeter of 1.53 miles.



Figure 5. North River Inlet (Scituate, MA) - Supported by Town of Scituate and Scituate Country Club; Partnered with UMass Amherst Geosciences Department

South River

The South River marsh site (Figure 6) is located in the town of Marshfield, and it is currently being used for an intensive study of sediment dynamics being conducted by a team of geologists from UMass Amherst. We installed 11 GCPs (blue markers) throughout the South River inlet. The full flight footprint covered 144 acres (outlined in blue) and had a perimeter of 3 miles. A reduced flight footprint (outlined in bright pink) covered 97 acres and had a perimeter of 1.96 miles.



Figure 6. South River Inlet (Marshfield, MA) - Supported by Town of Marshfield; Partnered with UMass Amherst Geosciences Department

Horseneck Beach

The marsh site at Horseneck Beach (Figure 7) is located in the town of Westport and contains portions of a salt marsh managed by MA DCR. This site was selected because it is a sentinel site being studied by MA Coastal Zone Management and appeared to be experiencing subsidence and inundation issues. We installed 9 GCPs (blue markers) throughout the Horseneck Beach marsh. The full flight footprint covered 131 acres (outlined in blue) and had a perimeter of 1.76 miles. A reduced flight footprint (outlined in bright pink) covered 100 acres and had a perimeter of 1.6 miles.



Figure 7. Horseneck Beach (Westport, MA) - Supported by MA Coastal Zone Management and MA Department of Conservation and Recreation (DCR)

Barnstable Great Marsh

The Barnstable Great Marsh study site (Figure 8) is located in a portion of the Barnstable Great Marsh in the town of Barnstable, and is managed by the Massachusetts Audubon Society. It was selected because it is a sentinel site being studied by MA Coastal Zone Management and it is largely unaffected by human land use impacts. We installed 8 GCPs (blue markers) throughout the Great Marsh. The full flight footprint covered 136 acres (outlined in blue) and had a perimeter of 2.13 miles. A reduced flight footprint (outlined in bright pink) covered 100 acres and had a perimeter of 1.86 miles.

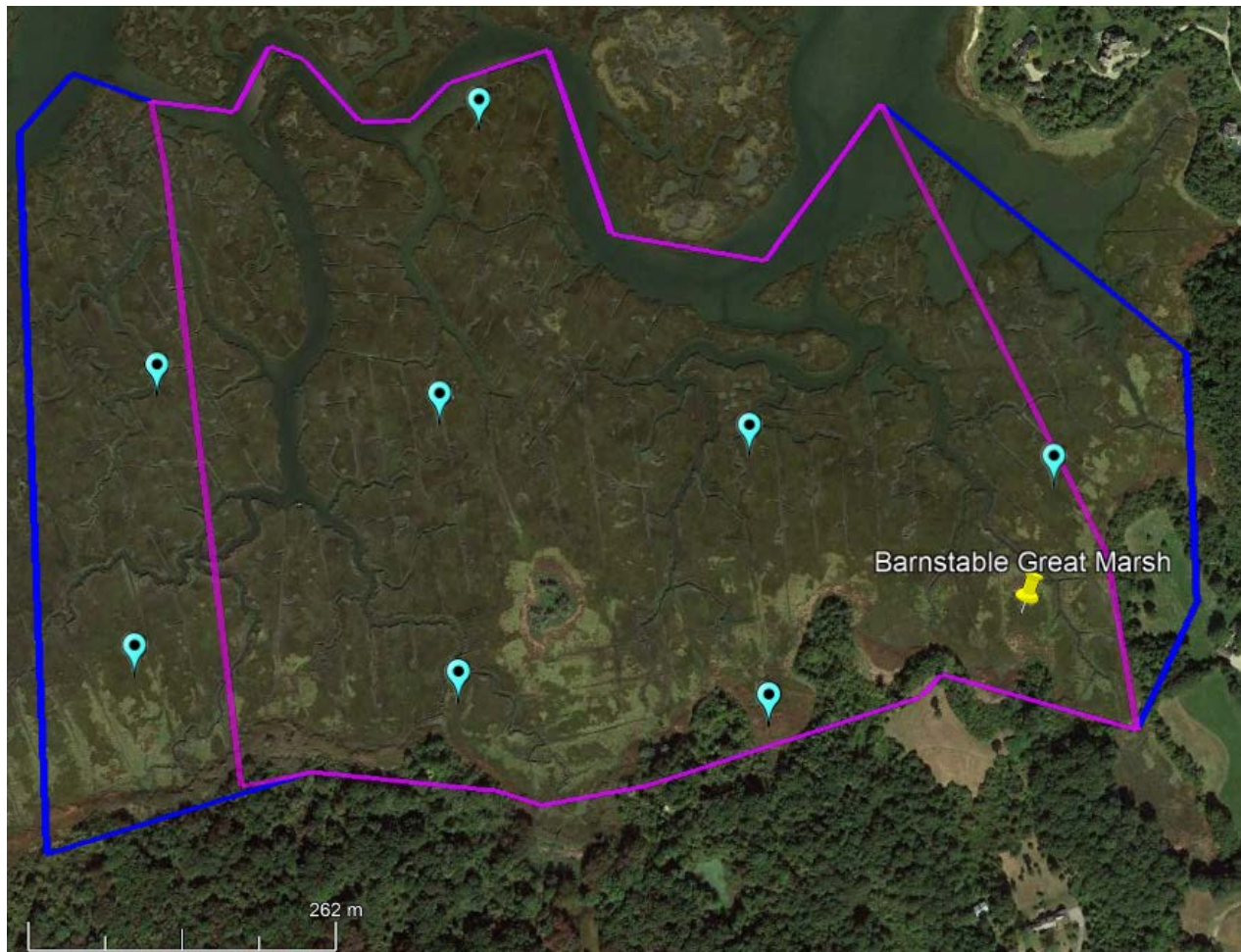


Figure 8. Barnstable Great Marsh Wildlife Sanctuary (Barnstable, MA) - Supported by the Massachusetts Audubon Society

Red River

The Red River marsh site (Figure 9) spans the Chatham and Harwich town line. It is managed by the Harwich Conservation Trust and the Chatham Conservation Commission. It was selected because of its proximity to a barrier beach, it contains a tidal restriction, has experienced restoration events, and appears to have interesting sediment dynamics. We installed 9 GCPs (blue markers) throughout the site. The full flight footprint covered 61.8 acres (outlined in blue) and had a perimeter of 2.43 miles. A reduced flight footprint (outlined in bright pink) covered 48 acres and had a perimeter of 2.15 miles. A reduced flight footprint was needed for this site to avoid flying over the cars entering the parking lot entrance.



Figure 9. Red River (Chatham and Harwich, MA) - Supported by Harwich Conservation Trust and the Chatham Conservation Commission

Wellfleet Bay Wildlife Sanctuary

This Wellfleet Bay Wildlife Sanctuary site (Figure 10) is located in the town of Wellfleet and is managed by the Massachusetts Audubon Society. This site was selected because it is a protected area that is experiencing extensive die back events and crab herbivory issues. We installed 10 GCPs (blue markers) throughout the Great Marsh. The full flight footprint covered 99 acres (outlined in bright pink) and had a perimeter of 1.83 miles. A reduced flight footprint was not needed for this area.



Figure 10. Wellfleet Bay Wildlife Sanctuary (Wellfleet, MA) - Supported by the Massachusetts Audubon Society

FLIGHT PREPARATION

Ground Control Points (GCPs)

Ground Control Points (GCPs) were installed in each salt marsh before conducting UAS flights and their locations documented by Real-time kinematic (RTK) positioning using a Trimble R10 RTK GNSS unit (Figure 11).



Figure 11. Ground Control Points being laterally and vertically located using a Trimble R10 RTK GNSS unit in Essex Bay. GCPs are 1'x1' PVC sheet board fitted with a ½" wide PVC pole that is inserted into the ground. A black 4" diameter circle is painted on the center of the board.

We used GCPs to constrain the reconstruction of multispectral orthomosaics and digital elevation models (DEMs), or in other words, to as accurately as possible spatially align these remote sensing digital products. This is a critical step to ensure that all aerial images for a site, representing particular multispectral bands (visible blue, green or red; rededge, near-infrared, and short-wave infrared), and representing particular points in time (e.g., date and point in the tide cycle) can be accurately stacked for analysis.

GCPs were strategically deployed such that each image captured by a sensor includes at least one GCP, or will be able to reference an area on the ground that overlaps at least one another image that contains a GCP. It took a substantial amount of effort to develop and test the appropriate design of these GCPs to ensure that they could withstand harsh weather conditions and remain in place, and team members doing image processing could see GCPs in images taken by all the spectral sensors used in this study. The

GCP design we settled on uses PCV Trim Boards with a painted black dot in the center for easier identification in the images. Each board was attached to a PCV pipe (not shown in Figure 11) that extends into the marsh platform to secure it in place.

The number of GCPs that are placed at each site varied and did not exceed 16 GCPs for a given site. GCPs are placed such that the distance between each row and column of GCPs is equal to 2 times the longest dimension of the image footprint of the Zenmuse X3, divided by the square root of 2 (Figure 12).

$$(GCP\ Spacing\ [m]) = (GCP\ Accuracy\ Drift\ Tolerance\ Factor) \times \frac{Image\ Footprint\ Width\ m^2]}{\sqrt{2}}$$

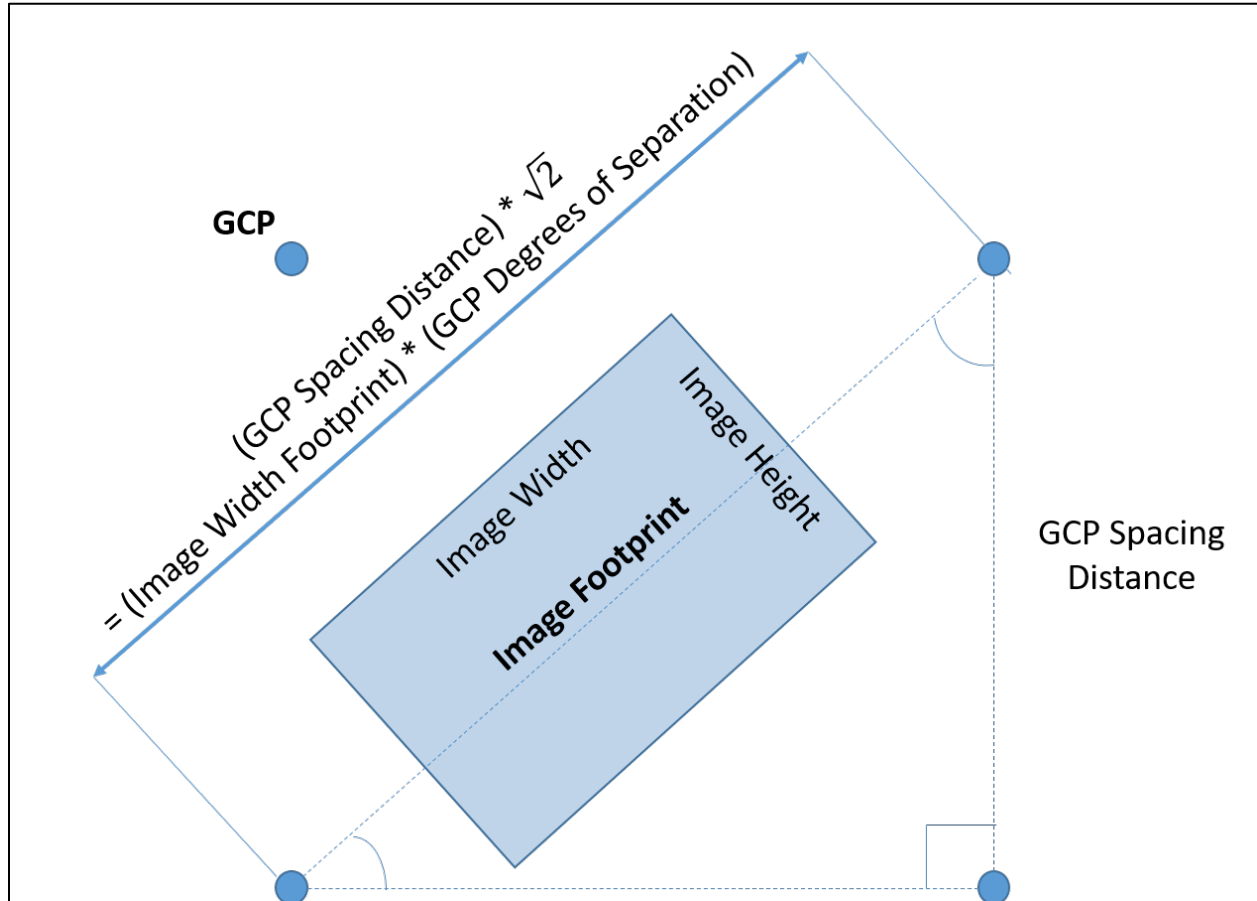


Figure 12. An illustration of GCP spacing distance.

At 122 meters the vertical footprint of the Zenmuse X3 camera – one of the sensors on our UAS machine -- is 159 meters, and the horizontal footprint is 211 meters. In order to guarantee that an adequate number of images captured by the Zenmuse X3 contains a GCP while the camera is in the nadir position, the GCPs were spaced in a grid pattern every 280 meters along each axis in a square grid pattern. The camera on our “Phantom 4 Pro” quadcopter has a similar but slightly smaller image footprint. GCPs placed along the perimeter of a site were spaced no more than half of that distance, 140 meters, from the site boundary. See QAPP Appendix A for more information about GCP spacing.

The lateral and vertical locations and location accuracies of the GCPs were measured with the Trimble R10 Real-Time Kinematic (RTK) Global Positioning System (GPS) at the beginning of each season. By using GCPs recorded with this GPS technology, we achieve horizontal accuracies of a few centimeters and vertical accuracies within 10cm. GCPs remained in place for the duration of the field season and were either cleaned and reused, or replaced prior to the first flight of the next field season.

Water Loggers

Water loggers were generally installed in the salt marsh before conducting the first UAS flight. We either placed our own water loggers (HOBO U20L or HOBO U20) at a site or used water-level measurements from another research group. Water loggers measured temperature and barometric pressure every 10 minutes. Barometric pressure was later converted into water depth using the HOBO Barometric Assistant package from the HOBOWare program.

Accurate water level readings relied on the current barometric pressure of the region at each data collection time interval. Either a HOBO U20L-01 water logger was installed in a dry upland area to measure barometric pressure every 10 minutes or we used barometric pressure data from a nearby weather station.

UAS FLIGHTS

Flights were conducted over the course of the 2018 – 2020 field seasons (May-November). Flights were conducted at low tide and high tide during spring tides, neap tides, and in between tides to capture maximum and minimum flooding extents. In some cases, mid tide was also captured. Data collected by sensors were used to train and test landscape classification models, develop hydrology models, and map flooding extent.

Flight parameters differed for each site and date based on weather, UAS availability, and camera/sensor availability (Table 1). Flight parameter calculations and additional details about each camera, sensor, aircraft, accessories, and our flight SOP can be found in QAPP Appendix A.

Table 1. Ground speed limits for each aircraft and camera combination given the certain parameters in QAPP Appendix A and a blur tolerance factor of 0.5.

Camera	Aircraft	Flight Speed Limit_Image Blur (m/s)	Flight Speed Limit_Image Trigger (m/s)	Flight Speed Limit_Aircraft (m/s)	Flight Speed Limit_Lower Limit (m/s)
SWIR 640	DJI Matrice 600	38.125	19.52	17	17
Micasense RedEdge M	DJI Matrice 600, Phantom 4 Pro	21.181	17.893, 20.333	17	17
Zenmuse X3	DJI Matrice 600	13.217	17.446	17	13.217
Phantom 4 Camera	DJI Phantom 4	16.721	17.08	14	14
Zenmuse XT 2 (LWIR)	Matrice 210	2.393	20.421	16	2.393
Zenmuse XT 2 (RGB)	Matrice 210	16.013	18.254	16	16

IMAGE PROCESSING

Software

The software used to process imagery was Agisoft Photoscan/Metashape.

Tagging Ground Control Points (GCPs)

“Tagging” GCPs was a critical step in creating accurate data products such as orthomosaics (composite imagery made from all the aerial imagery collected in one flight) and digital elevation models (DEMs). For each flight, one of our image processing team members had to locate and mark in Agisoft Photoscan/Metashape the very center of the GCPs in every spectral image (“band”) that contains a GCP. For example, if one image captured by the MicaSense sensor included a GCP, the analyst tagged the GCP in the visible blue, green and red images, as well as in the red-edge, or near-infrared bands. Despite our best efforts to create GCP markers detectable by all sensors, occasionally in the red edge, near-infrared or short-wave infrared imagery, the GCPs were challenging to locate and tag. In these instances, for geo-referencing quality control, our rule was that the analyst could not continue onto other image processing steps until the average error in tagging each GCP across bands was < 8 cm.

RGB Orthomosaics and Digital Elevation Models

Multispectral orthomosaics and DEMs are created in Agisoft Photoscan according to the workflow listed in QAPP Appendix A.

The images from flights taken by our Zenmuse X3 sensor were used to develop a high-resolution RGB orthomosaic and a high-resolution Digital Elevation Model (see Data Products section below) for each site. Images taken with the MicaSense RedEdge M were used to develop a 5-band multispectral orthomosaic of reflectance values for each time period (stage in the tide cycle) that images were captured on that date. Images taken with the SWIR 640 were used to develop a single band orthomosaic of reflectance values for images captured at each time period on that date.

Images from the MicaSense RedEdge M and SWIR 640 were calibrated to provide actual light reflectance values for the bands (visible blue, green and red, red edge, near infrared and shortwave IR) rather than simple “digital numbers,” representing color like the products of traditional digital cameras. This means the pixel values in each image represents a scientific measure of emitted light in that range of the electromagnetic spectrum. The calibration process uses data from the reflectance panel images and the sun sensor data. Once images from our sensors were calibrated, they were aligned based on GCP tagging and are used to build dense clouds and higher-level products similar to the workflow of the Zenmuse X3. More details about image processing can be found in QAPP Appendix A.

Quality Control

Procedures outlined in QAPP Appendix A and Appendix B were followed to maintain the highest standards for image acquisition, image processing, and interpretation.

In order to maintain the highest standards of multispectral image and multispectral reflectance quality, the spectral calibration procedures outlined in QAPP Appendix A section 8.1, and the Micasense RedEdge M and SWIR 640 calibration steps outlined in the preflight procedure in 9.3.1 were followed. Additionally, flights were conducted so primary flight transects were perpendicular to the sun’s azimuth to ensure best lighting geometry for image acquisition. After each flight, images were uploaded to the field computer and checked to ensure that image capture was successful.

Procedures in QAPP Appendix A section 9.5 were followed to maintain consistent quality of orthomosaic and DEM reconstruction. Important quality control components of our image processing protocol included removing all photos less than 0.65 in image quality (with exceptions), developing low-accuracy and highest accuracy alignments, importing and tagging GCPs in each band with a maximum allowable error, executing realignments, as well as developing a dense cloud, a mesh, and an orthomosaic on highest reconstruction settings.

PHOTO INTERPRETATION FOR CREATION OF A BASE MAP FOR GROUND DATA COLLECTION

In order to model salt marsh classification (classes and subclass) and stressors (classification attributes) it is necessary to collect ground-based field data to train and validate the models. The purpose of photo interpretation is to use the RGB orthomosaics to inform the placement of transects for on-the-ground data collection. A photo interpreter reviewed each orthomosaic and identified patches of vegetation, bare ground and water likely to correspond to the classes and subclasses in our classification scheme (see below). The interpreter then created a series of “ricocheting transects” that would intersect as

many of the different classes and subclasses as possible (Figure 13). For more information see QAPP Appendix B.

Field crews used ricocheting belt transects to characterize salt marshes using a non-random, stratified sampling approach. A non-random approach was used because it accounted for ease of access, provided an efficient approach to data collection, made it possible to achieve adequate representation of all classes and subclasses, and helped reduced impacts to marsh vegetation and substrate.

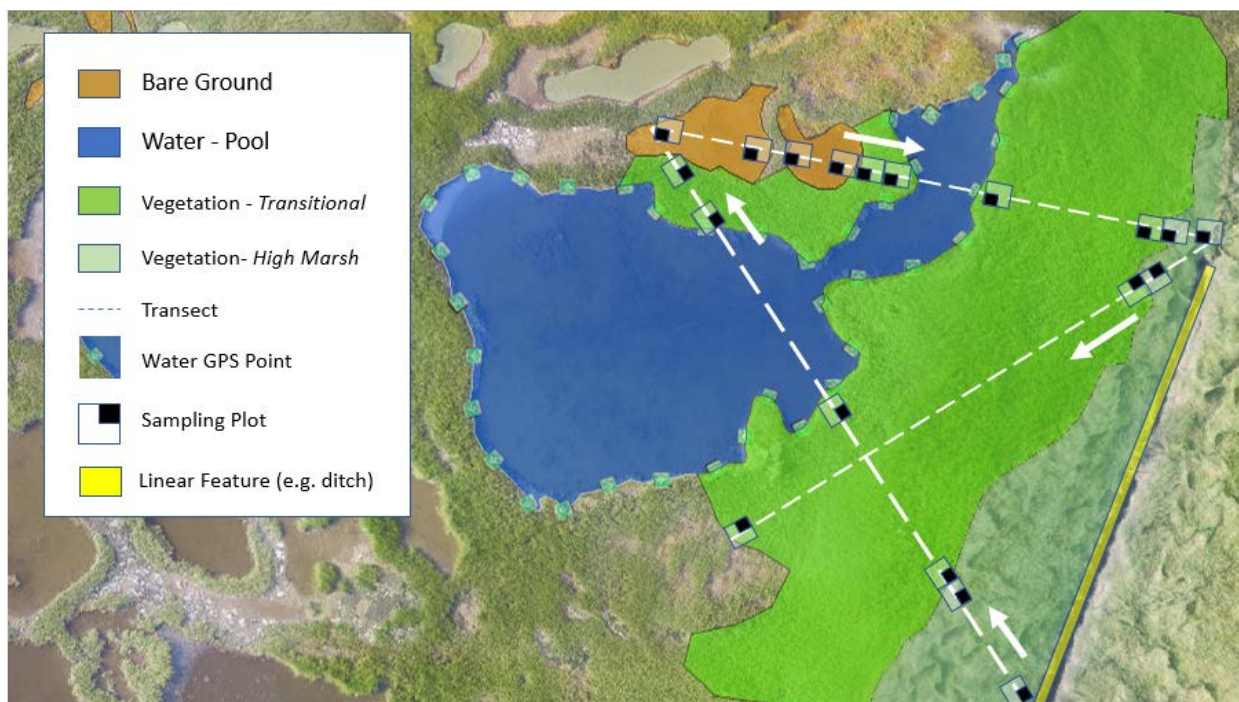


Figure 13. Visual approach to sampling salt marsh landscape at the subclass level. The dashed line represents a ricocheting belt transect that intersects a diversity of classes and subclasses. Aerial photo is of a salt marsh in Rowley, Massachusetts.

ON THE GROUND DATA COLLECTION

The ground-based field data collection protocol can be found in QAPP Appendix C. Before heading to the site, the field manager and field assistants confirmed that all necessary permissions had been secured for parking and accessing the salt marsh. Once at the site, the field crew used the predetermined 2m wide ricocheting belted transects to guide data collection. A main goal of the ricocheting transect placement was to capture sufficient replicates for a diversity of classes, subclasses, and attributes using a 4m² minimum plot unit. A Trimble R10 RTK GNSS receiver was used to measure the start and ending points of each subclass along the transect. The edges of water features were generally documented using a delineation approach instead of ricocheting transects. A classification scheme (see below) lists how the field crew recorded every plot's class, subclass, and attributes in the RTK unit and on data sheets. The lateral and vertical accuracy of validation points were subject to the same accuracy requirements outlined in Appendix A, section 8.2.

CLASSIFICATION

Salt marsh sampling plots were classified using the classification scheme described in QAPP Appendix E. Field crews recorded the transect number, plot number, class, subclass and all attributes associated with the plot being sampled. The objective of the classification scheme was to have a code made of numbers and letters that could describe every type of landscape cover in a 4m² plot that could be observed in a New England salt marsh. In total, there were 15 vegetation subclasses, seven water subclasses, three bare ground subclasses, and 20 descriptive attributes.

Modifications

Over the course of three years of this phase of the project, we only made six modifications to the original classification scheme. These modifications were: 1) expanding subclass “01” to include 70%+ of tall form *Spartina alterniflora* rather than 90%, 2) adding subclass “13” to denote linear vegetated ditch edges that have a mix of *S. alterniflora* and high marsh species, and would later be turned into polygons, 3) adding a subclass “14” to denote a notable presence of a flowering white clover species mixed with high marsh species, 4) adding subclass “15” to denote areas of macroalgae fixed to the substrate of shallow water features, 5) adding attribute “s” to denote sediment deposits, and 6) and adding attribute “t” to denote presence of trash/debris.

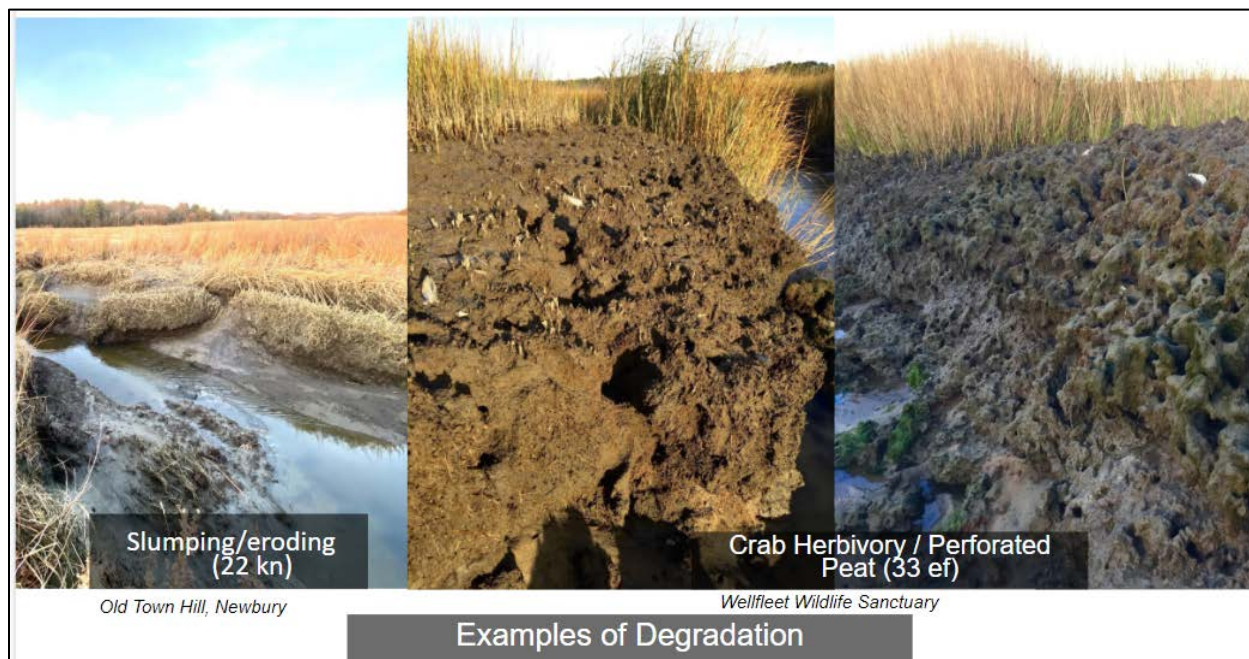


Figure 14: Examples of using the classification scheme to denote 4m² areas of slumping and eroding creek edges (22 kn) and bare areas with perforated peat and crab herbivory (33 ef).

Salt Marsh Classification

Minimum mapping unit (scale of the threats/vulnerability, phenomena)

Polygons: 2m x 2m, 4 sq m

Linear: 0.5 m x 3 m

First Level: Class (first digit - number)

- 1 - Vegetated: > 30% vegetation cover
- 2 - Water feature: 100% inundated at typical high tide with < 30% vegetation cover
- 3 - Bare ground: Exposed at typical high tide with < 30% vegetation cover

Second Level: Subclass (second and third digits - numbers)

- 1 - Vegetated: > 30% vegetation cover
 - 01 - Low marsh (tall form *Spartina alterniflora* dominant): > 70% plant cover in tall form *S. alterniflora*
 - 02 - Intermediate marsh (mix of high marsh vegetation and tall form *S. alterniflora*): high marsh species dominant with 5-40% tall form *S. alterniflora*
 - 03 - Transitional marsh 1: short form *S. alterniflora* dominant (> 80%) mixed with typical high marsh species
 - 04 - Transitional marsh 2: short form *S. alterniflora* common or dominant (30-80%) mixed with typical high marsh species
 - 05 - Transitional marsh 3: *S. patens* & *D. spicata* dominant but mixed with 5-30% short form *S. alterniflora*
 - 06 - High marsh 1: > 90% plant cover in *S. patens* & *D. spicata* and < 5% short form *S. alterniflora*
 - 07 - High marsh 2: < 90% plant cover in *S. patens* & *D. spicata*, mixed with other high marsh species but < 10% shrub species and < 5% short form *S. alterniflora*
 - 08 - *Juncus gerardii* band: > 50% of marsh vegetation is *Juncus gerardii*
 - 09 - Salt-shrub marsh (high marsh vegetation mixed with shrub species): *S. patens* & *D. spicata* mixed with > 10% *Iva frutescens*, *Limonium carolinianum*, *Baccharis Halimifolia*
 - 10 - *Salicornia* or *Suaeda* marsh: > 30% areal coverage and > 50% vegetative cover of *Salicornia* spp. and/or *Suaeda* spp.
 - 11 - Brackish marsh: 50% of vegetative cover of brackish marsh species (e.g. *Schoenoplectus* spp., *Bolboschoenus* spp., *Typha* spp.)
 - 12 - Brackish marsh - *Phragmites*: > 30% vegetative cover of *Phragmites australis*
 - 13 - Vegetated ditch edges: mix of high marsh vegetation and intermediate form (neither tall nor short) *Spartina alterniflora* as linear features along the edges of water features (typically along the crown of ditch banks)
 - 14 – High marsh vegetation mixed with a flowering white clover species
 - 15 – Macroalgae fixed to the substrate of a shallow water feature

- 2 - Water: 100% inundated at typical high tide with < 30% vegetation cover
 - 21 - Ditch: linear feature, straight lines often in a grid formation
 - 22 - Natural creek: linear feature, branching and meandering
 - 23 - Dug runnel: linear feature, ditch-like, but shallower (6" - 12")
 - 24 - Excavated sinuous creek: linear feature, like a natural creek but excavated, not natural
 - 25 - Panne/pool: polygon feature, not associated with ditches or evidence of excavation (spoil piles)
 - 26 - Artificial pool: polygon feature, associated with ditches or with evidence of excavation or berms/dikes
 - 27 - Unvegetated bank: sloped topography on low marsh substrate in regularly flooded, intertidal zone
- 3 - Bare ground: exposed at typical high tide with < 30% vegetation cover
 - 31 - High marsh substrate - deposition: < 30% living vegetation due to the presence of overwash or ice rafted soil deposition on high marsh substrate in an irregularly flooded zone
 - 32 - High marsh substrate - wrack: < 30% living vegetation due to the presence of wrack/debris accumulation on high marsh substrate in an irregularly flooded zone
 - 33 - High marsh substrate - dieback/deinundated: bare ground on high marsh substrate in irregularly flooded zone

Third Level: Attributes (fourth digit - letter)

- a. Healthy vegetation: < 30% of vegetation shows any indication of stress (discoloration, unusually stunted growth, thinning, foliage damage, wilting)
- b. Stressed vegetation: > 30% of vegetation shows any indication of stress (discoloration, unusually stunted growth, thinning, foliage damage, wilting)
- c. Cropped vegetation: > 30% of vegetation affected by herbivory
- d. Algal mat: > 50% of surface covered with matted algae
- e. Perforated peat: > 25 crab burrows per square meter
- f. Low density peat: marsh peats demonstrates significantly less resistance to probing than healthy peat (greater amount of peat volume is air or water)
- g. Slumping/eroding: > 50% of the area show indications of erosion or slumping
- h. Hypersaline: indicators of hypersalinity, based on vegetation and salt deposits, are present
- i. Artificially elevated: substrate, whether vegetated or not, has been anthropogenically elevated by the deposition of spoil or other material forming linear berms within the salt marsh
- j. Water at low tide: water feature holds water throughout a typical tide cycle
- k. Dewatered at low tide: water feature does not hold water at low tide during a typical tide cycle

- l. Tidal flat: flat topography located in regularly flooded, intertidal zone
- m. Maintained: artificial water feature (ditch, runnel, excavated sinuous creek, artificial pool) has been recently constructed or maintained
- n. Non Maintained: artificial water feature (ditch, runnel, excavated sinuous creek, artificial pool) has does not appear to have been recently constructed or maintained
- o. Excavated pool: artificial pool was created by excavation
- p. Impounded pool: artificial pool was created by impoundment (including ditch plugs)
- q. OMWM: water feature is part of an Open Marsh Water Management system
- r. Widening: Water feature appears to be widening
- s. Sediment deposit: naturally deposited sediment that reduces the aerial coverage of vegetation, either temporarily or permanently, by >20%
- t. trash/debris washed onto the marsh that reduces the aerial coverage of vegetation, either temporarily or permanently, by >20%

Table 2. Attributes and applicable classes in the salt marsh classification system.

Attribute	Vegetated	Water feature	Bare soil
a. Healthy vegetation	X	X	
b. Stressed vegetation	X	X	
c. Cropped vegetation	X	X	X
d. Algal mat		X	X
e. Perforated peat	X	X	X
f. Low density peat	X	X	X
g. Slumping/eroding	X	X	X
h. Hypersaline	X	X	X
i. Artificially elevated	X	X	X
j. Water at low tide		X	
k. Dewatered at low tide		X	
l. Tidal flat		X	
m. Maintained		X	
n. Unmaintained		X	
o. Excavated pool		X	
p. Impounded pool		X	
q. OMWM		X	
r. Widening		X	
s. Sediment deposit	X	X	X
t. Trash/Debris	X	X	X

ANALYZING REMOTE SENSING DATA

The ricocheting transect field data collected for this project (see QAPP Appendix C) were used as model reference training and validation data for individual sites. In order to generate training data for the model, the transect sampling plot data (see above, Figure 13) in the form of comma delimited value (CSV) files were transformed using GIS functions into ArcGIS “shapefiles” in the form of polygons representing 4m-wide belt transects. The salt marsh classification levels are table headers in each shapefile; this includes salt marsh classes, subclasses, and attributes (see QAPP Appendix E) along with other metadata. The polygons were used for processing remote sensing data described below to locate pixels for use in land cover classification training and validation. The production of these polygons based on field transect plot data for any site is a time consuming process when done manually. Consequently, we automated the process using the programming language Python and documented it using “Jupyter Notebook” so that the process can be easily replicated for multiple days of collection across multiple sites. Details of this process are described in QAPP Appendix D.

For individual salt marsh sites, classification models were run with all available spectral orthomosaic imagery. This included all stages of tide cycles and all spectral bands. A suite of classification outputs were produced for this project and not all imagery were required or appropriate for creating each particular product. For example, model classification of salt marsh vegetation subclasses is performed with all available low-tide imagery and model classification of bare ground and water subclasses are performed with high-tide imagery. This flexibility yielded the ability to customize the classification model to fit the needs of the individual product/output.

Quality Control

Several procedures were followed to ensure UAS images taken at different time points could be used concurrently as model variables/attributes. See QAPP Appendix D to learn how we addressed spatial alignment, image quality, and shapefile standards.

RESULTS

OVERVIEW OF WORK COMPLETED

UAS Flights

By the end of Fall 2020, we had collected data over three field seasons. In total, we have executed 149 flights at nine sites that have a combined area of 1,259 acres of salt marsh habitat. This amount of diverse spectral and hydrological data were enough to execute desired spatial and temporal analyses. Spectral data were collected during every flight using either an RGB (Phantom 3, Phantom 4 Pro, or Zenmuse XT2), MicaSense RedEdge, and/or SWIR (short wave infrared) sensor. Flights were conducted at different tidal stages (low tide, mid tide, and high tide). A tally of flights by location, tidal stage, and sensor is presented in Table 3.

Table 3. Number of UAS flights by location, tidal stage, and sensor used for the 2018-2020 field seasons.

			Newbury	Essex Bay	Peggotty	North River	South River	Westport	Barnstable	Red River	Wellfleet
Number of Flights (as of 2020)	Tide	Total	27	28	31	7	3	19	1	23	10
	High	SWIR_H	1		2	1		1			
		RedEdge_H	6	7	5	2	1	6		3	3
		Zenmuse_H			2				1	2	
	Mid	SWIR_M	2	1	3	1		2		1	2
		RedEdge_M	6	5	7	1		3		3	1
		Zenmuse_M	1	2	6					7	
	Low	SWIR_L	1	1		2	1			1	1
		RedEdge_L	9	8	4	3	2	5		4	3
		Zenmuse_L		1				2		2	

In general, we collected more spectral data during low tides and high tides than mid tides. As expected, more total flights have been conducted at sites that were part of our first field season in 2018 than sites added in 2019. Significantly fewer flights were conducted at 1) Barnstable Great Marsh, due to frequent low-flying planes and difficulty accessing the site with gear in tow, and 2) South River, due signal interference when ground-truthing and tightly clustered residential properties making flight patterns difficult to execute.

Ground Truthing

Land cover ground-truthing data were collected at all nine sites. Most of the data collection focused on vegetation and delineating the perimeter of water features. Details on the number of plot points taken for each subclass by site are presented in Table 4. In total, we collected data for 3,138 plot points across the nine sites. It is important to note that the total number of plot points is not directly related to the number of training and validation pixels available for each subclass, because the total area covered by

belt transects between two plot points can span from a few meters to up to 50 meters. In other words, there are many more training and validation pixels than there are plot points because of the ricocheting belt transect approach and the creation of 4m wide polygons of particular land cover classes using start and end points along the transect. Total area covered for each subclass were calculated after ground truthing data were converted into shapefiles (see QAPP Appendix D for details).

Table 4: Total number of ground truthing points collected at each site by subclass.

		Sites								
	Subclass	Barnstable	Peggotty	North River	Wellfleet	Newbury	Essex	Westport	Red River	Total
Vegetation Types	01	35	44	54	75	36	20	11	51	326
	02	38	18	39	23	38	24	8	18	206
	03	23	17	20	33	16	19	49	57	234
	04	40	15	7	1	17	24	0	35	139
	05	9	16	2	0	11	8	0	8	54
	06	74	50	32	29	76	62	0	20	343
	07	0	0	4	5	0	6	0	8	23
	08	17	5	11	0	2	0	0	4	39
	09	8	9	3	1	11	0	0	51	83
	10	0	15	12	33	7	4	0	9	80
	11	28	8	0	10	0	0	0	47	93
	12	10	12	10	6	0	36	5	43	122
	13	42	24	6	0	6	0	0	0	78
	14	0	0	6	0	0	0	0	0	6
Water Features	21	41	23	46	0	12	45	0	0	167
	22	53	36	50	0	44	29	73	0	285
	23	0	6	0	0	24	0	18	0	48
	24	0	0	18	0	0	0	0	0	18
	25	21	153	19	4	15	267	118	13	610
	26	0	0	0	0	6	0	0	0	6
	27	0	3	2	0	1	0	0	0	6
	28	0	10	0	0	0	0	0	0	10
Bare	31	2	12	7	0	0	12	0	9	42
	32	0	2	15	20	0	0	5	5	47
	33	3	0	8	40	0	13	0	9	73
	Total	444	478	371	280	322	569	287	387	

Our sites cover a range of elevations (Figure 15). The two sites at the lowest elevations - Red River and Westport - are located along the southern coastline of Massachusetts. Our data show that subclasses occurred at different elevations across the nine sites. This prompted us to consider whether inundation frequency and/or duration better explains the presence or absence of a certain subclass rather than elevation above mean sea level.

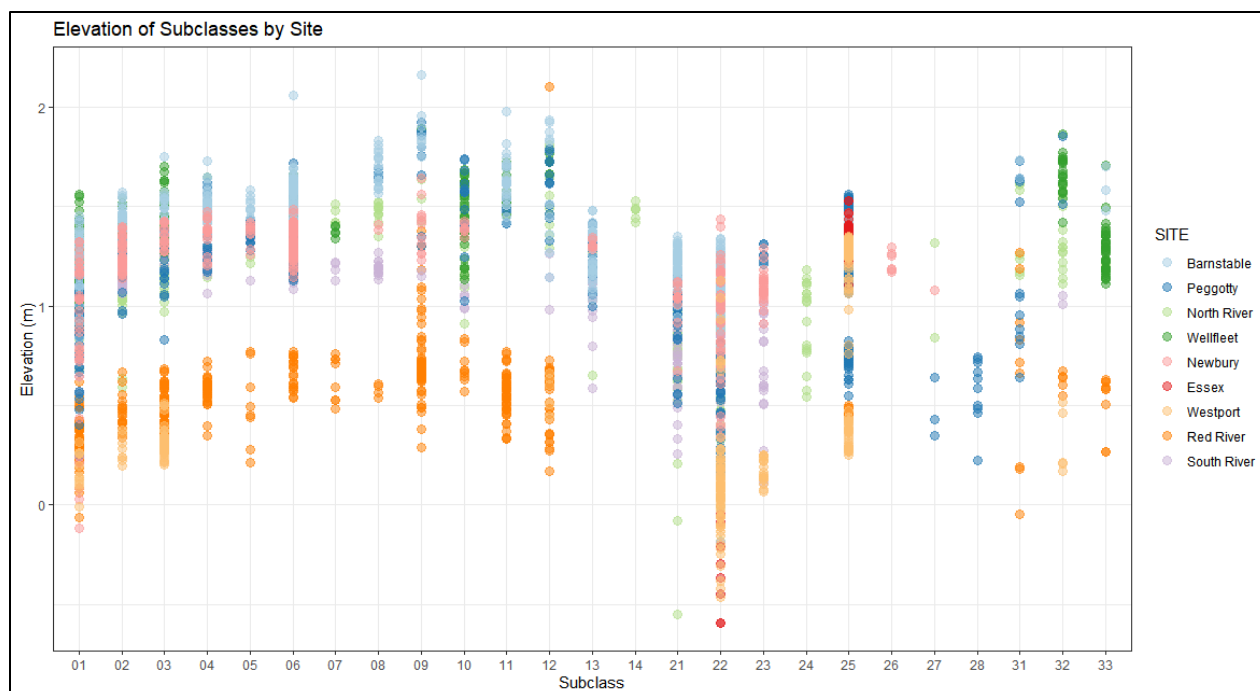


Figure 15. The range of elevation heights (in meters) of each subclass colored by site.

Hydrology

We collected hydrology data from all nine sites during at least one of the three field seasons. Hydrology data collected by MA CZM were used for the Essex Bay, Barnstable, and Horseneck Beach sites. For each site we had at least one water logger located at the bottom of a creek channel, and each logger's location and elevation was surveyed with respect to the North American Vertical Datum 1988 (NAVD88). The water loggers are set to record the water level above their location every 10 minutes and were calibrated for changes in atmospheric pressure either using a secondary logger that is above the flooding level of high tides or using a proximate NOAA weather station. This allowed us to record the water level within the marsh at virtually any point in time during the three field seasons (2018-2020). See Figure 16 for an example of data obtained from the water logger.

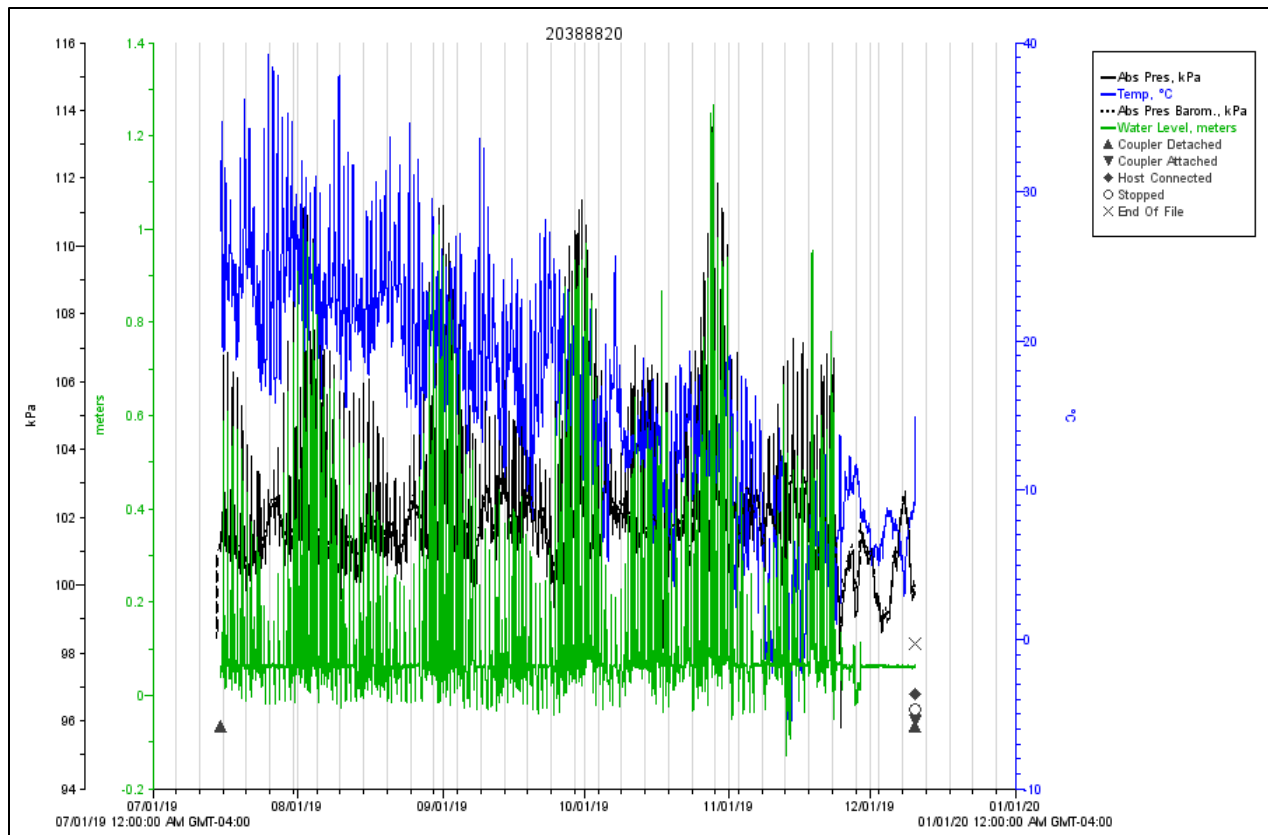


Figure 16: Graph showing the barometric pressure (black), water temperature in Celsius (blue), and water level (m) (green) every 10 minutes at Wellfleet Bay Wildlife Sanctuary for the 2019 field season.

DATA PRODUCTS

True Color (RGB) Orthomosaic

True color orthomosaics were developed using the visual Blue, Green, and Red sensor images provided by the Phantom 4 Pro camera or the Zenmuse X3 on our Matrice 600 unoccupied aerial vehicle (UAV). These orthomosaics are made up of thousands of photos accurately stitched together in a process informed by the GCP tagging process. An accurate orthomosaic allowed us to identify features at the subclass and even attribute level, and was used to guide the placement of ricocheting transects. Orthomosaics can be visually compared on a seasonal or annual basis to identify surface changes in water features, bare ground, and vegetation subclasses. See Figure 17 for an example of a “true color” visible Red, Green and Blue (RGB) orthomosaic.



Figure 17. A low tide orthomosaic of the Red River site in Chatham and Harwich MA. Imagery captured in RGB with a DJI Phantom 4 Pro camera.

Digital Elevation Models (DEMs)

Through the Agisoft Photoscan photogrammetry process, Digital Elevation Models (DEMs) were created for each site (see Figure 18 for an example). These products represent the elevation of the surface of the vegetation canopy, water, or exposed soil. It is not the same as a Digital Terrain Model, representing the elevation of the land surface or the marsh 'platform'. In this report, we will just use the phrase DEM because those products represent the elevation of the land cover surface.

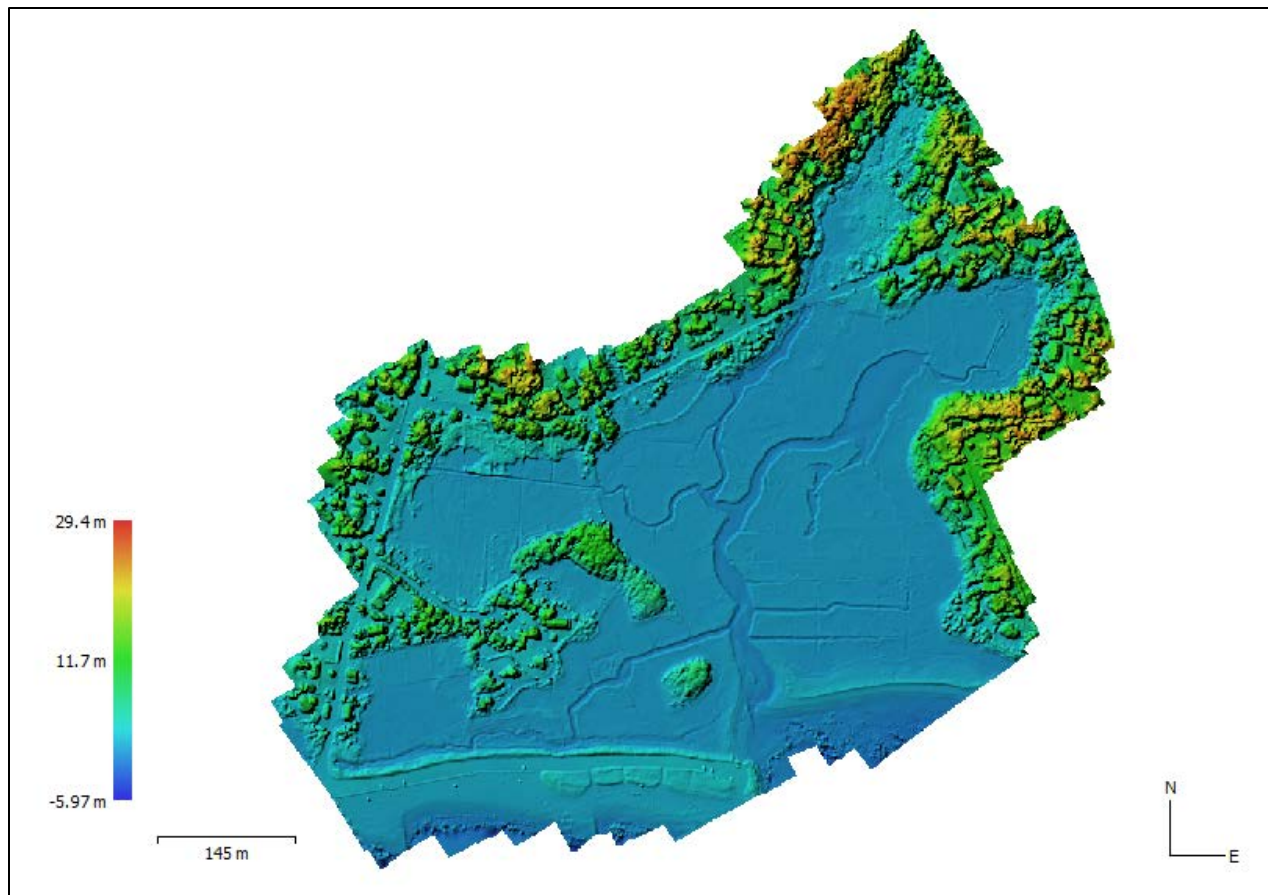


Figure 18. A low tide DEM of the Red River marsh, Chatham and Harwich, MA. Imagery captured in RGB with a DJI Phantom 4 Pro camera.

The root mean-square error (RMSE) for the GCPs that we used to reconstruct an orthomosaic or DEM had to be less than or equal to ground-sampling distance for camera images used for that reconstruction. We developed DEMs from the highest resolution camera available. For DEM's produced with a Phantom 4 Pro the tolerance for the RMSE is 3.3 centimeters, whereas DEM's or Orthomosaics produced with a Micasense RedEdge M camera have tolerance for the RMSE of 8.3 cm.

The most significant error in the DEM products we produced came from the fact that the images used in the DEM reconstruction do not penetrate the canopy of vegetation cover and thus, measure the elevation of the vegetation cover and not the underlying terrain. In other words, the data represent the elevation of vegetation or other exposed land cover – a digital surface model – rather than the earth surface underneath vegetation canopy, referred to as a Digital Terrain Model. This can make it difficult to understand flooding patterns strictly from the photogrammetry-derived DEMs. As Table 5 shows, this error varies significantly depending on the land cover class and subclass. Areas with low vegetation growth or no vegetation, such as class 31 (bare ground) and class 22 (creek channel), tend to have very low altitudinal errors in the DEM, whereas areas where vegetation tends to grow relatively tall, such as Class 12 (*Phragmites*), have larger altitudinal errors in the DEM. Error was calculated by taking the difference between the measured elevation with an RTK GNSS receiver and the elevation indicated in the DEM at that corresponding location.

Table 5. Summary statistics for the elevation errors by class at the Red River site; specifically the mean, standard deviation, median, minimum, and maximum error. Error is calculated by taking the difference between the measured elevation with an RTK GNSS receiver and the elevation indicated in the DEM at that corresponding location.

Class	Sample Count	Mean (m)	Standard Deviation (m)	Median (m)	Min (m)	Max (m)
33	8	0.076	0.057	0.059	0.006	0.178
32	5	0.203	0.039	0.187	0.161	0.251
31	8	-0.006	0.046	-0.005	-0.093	0.050
22	25	0.161	0.166	0.112	-0.092	0.561
12	40	0.344	0.725	0.468	-2.105	1.601
11	42	0.500	0.214	0.464	0.178	1.193
10	2	0.090	0.134	0.090	-0.005	0.185
9	46	0.249	0.147	0.225	0.010	0.598
8	4	0.188	0.043	0.179	0.145	0.248
7	4	0.237	0.092	0.244	0.122	0.341
6	11	0.182	0.057	0.180	0.090	0.294
5	8	0.313	0.155	0.355	0.099	0.538
4	28	0.192	0.077	0.181	-0.023	0.321
3	42	0.221	0.106	0.208	0.040	0.479
2	13	0.261	0.096	0.233	0.132	0.506
1	40	0.385	0.222	0.377	0.049	0.982
ALL	326	0.281	0.312	0.245	-2.105	1.601

Temporal Changes in Elevation

We used the Agisoft software environment to compare the DEMs constructed from low tide flights. By comparing the fine-scale DEMs every year, we identified which areas within a salt marsh were experiencing a loss or gain in elevation (Figure 19). It is important to remember that our current DEMs represent digital surface models (DSMs) because elevation measurements are based on the surface of

the vegetation canopy. Therefore, we feel more confident in elevation change measurements identified in dewatered creeks or areas of bare ground at low tide rather than within vegetation subclasses. In future work, we intend to explore the possibility of producing DEMs that are closer to digital terrain models (DTMs) by including adjustment factors based on RTK elevation data from the on-the-ground data collection or by using data from flights at low tide prior to the seasonal “green-up” in May.

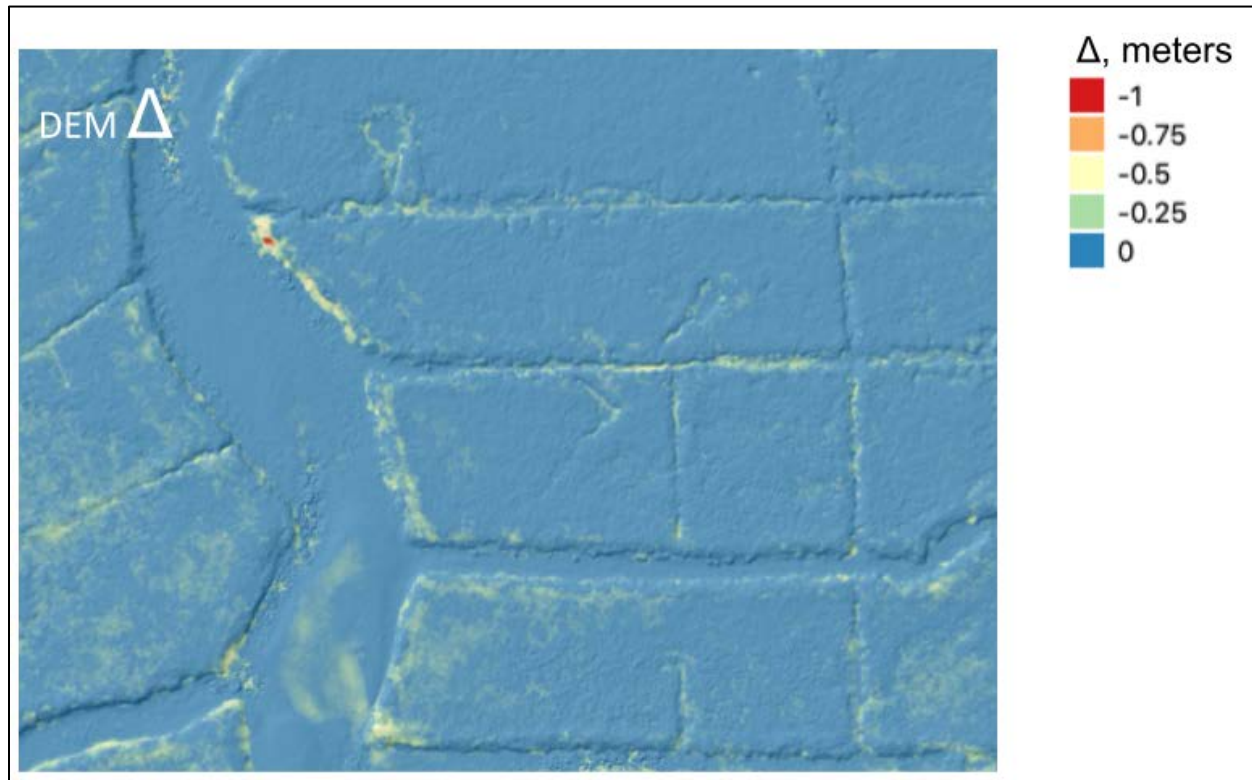


Figure 19: The results of a change in elevation analysis conducted in Agisoft. The output suggests that there are areas along Red River’s creek edge and the platform edge that have decreased in elevation by approximately a half a meter (colored light yellow) between a low tide flight conducted in 2019 and a low tide flight conducted in 2020. There is also one area that appears to have decreased in elevation by approximately one meter.

Inundation Mapping

Water logger data combined with the multispectral data collected from the UAS flights, provided information that we used to conduct several analyses with potential to provide detailed characterization of salt marsh tidal hydrology. Using the multispectral data, we used the Near Infrared (NIR) and/or the Short-wave Infrared (SWIR) images or “bands” to distinctly map the water extent at different tidal stages; water appears extremely dark and opaque in these bands, whereas vegetation and sediment appear much brighter, thus providing excellent contrast between regions that are inundated and not inundated (see Figures 20 & 21 for examples). The boundaries of inundation can then be compared to the DEM to infer the water elevation.

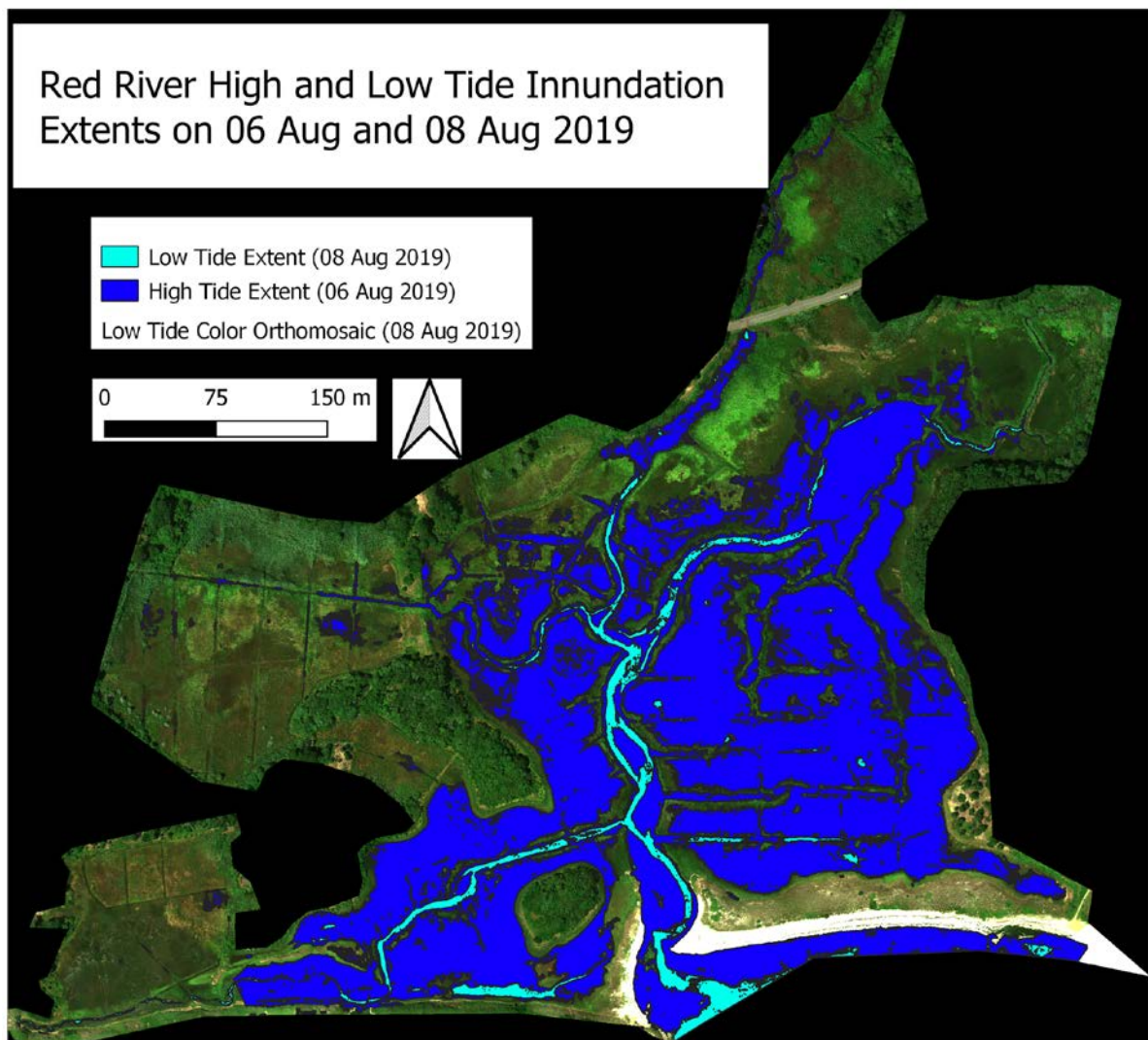


Figure 20. The extent of inundation at the Red River site for low tide on 08 August 2019 (light blue) and for high tide on 06 August 2019 (dark blue) as measured by the darkened regions in the NIR band.

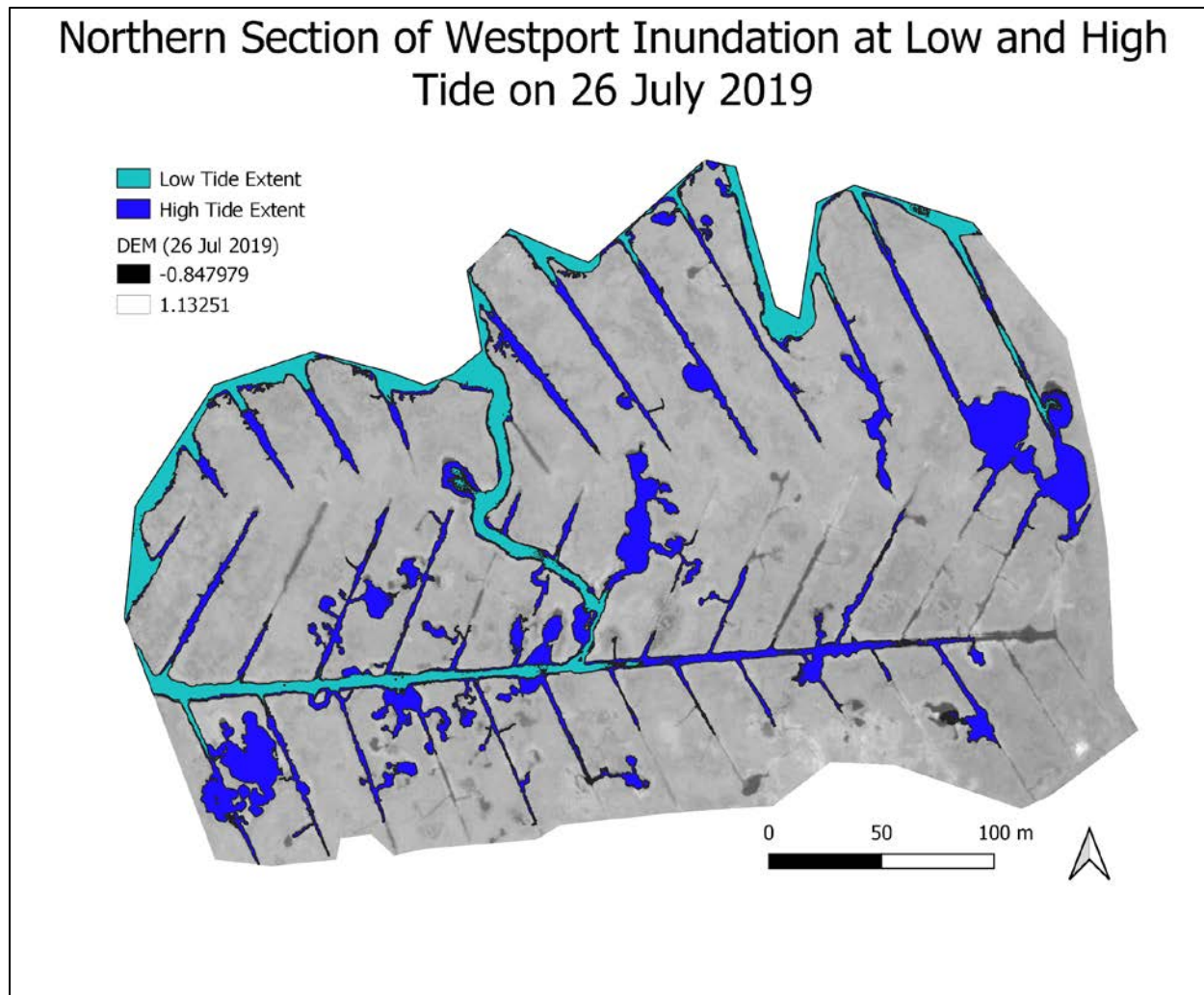


Figure 21. The inundation extent of a northern section of the Westport marsh site at both low tide (light blue) and high tide (dark blue) on 26 July 2019 as measured by the darkened regions in the NIR band.

Being able to measure the water level *in situ* with water loggers and with remote sensing techniques, in theory, should allow us to confirm the accuracy of remote sensing techniques to assess water level and inundation extent. Once appropriate techniques for inferring the water level from remotely sensed data are established, remote sensing data can then be used to define lines of elevation at varying tidal stages within the salt marsh to further refine the digital terrain model (Figure 22).

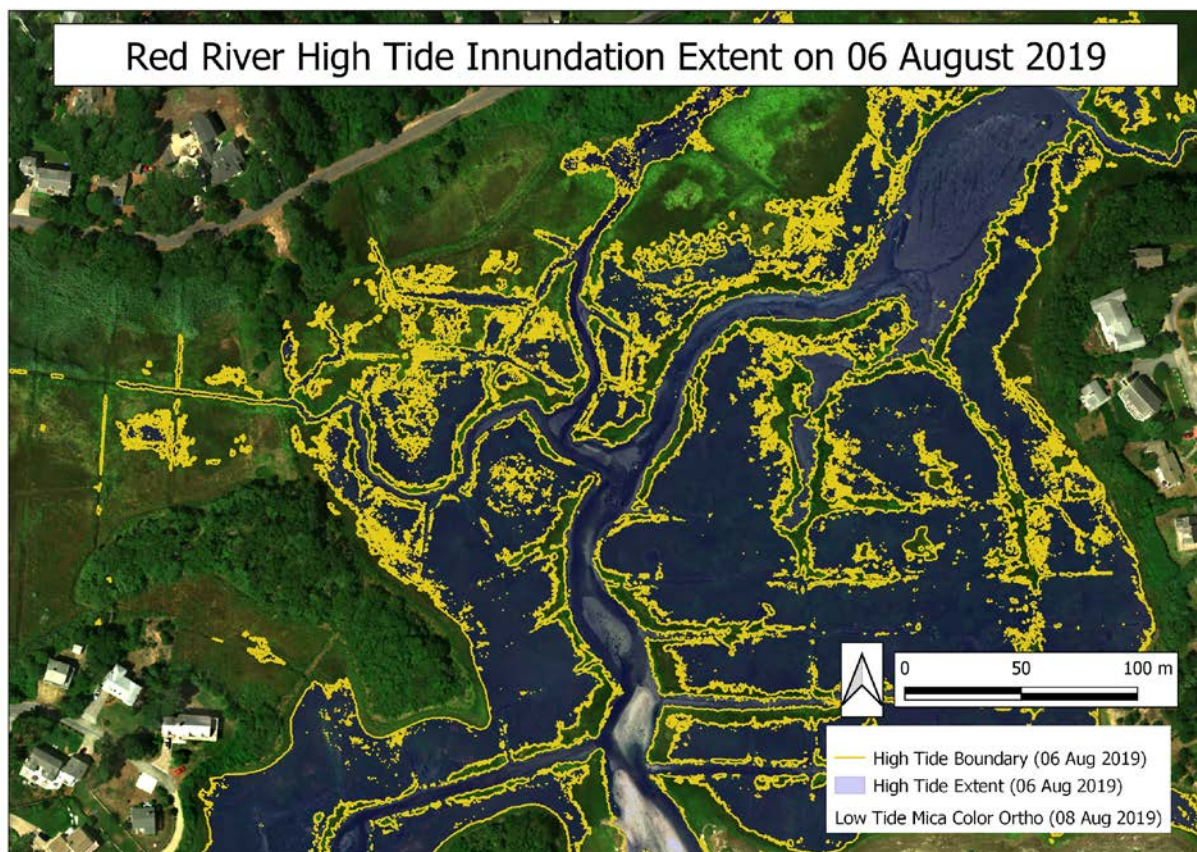


Figure 22. The boundary of the inundation extent as measured by the NIR band at high tide on 06 August 2019 is indicated by the yellow line. The elevation values of the DEM at a sampling of points along these lines provide a means to estimate the water elevation.

Development and refinement of these techniques is ongoing. In the case of high tide on 06 August 2019 (Figure 22), we found a significant discrepancy between the water elevation as inferred from remotely sensed data and the elevation measured with the water logger. In the case of 26 July 2019 at Westport (Figure 21), however, there was close agreement between the elevation inferred from our remotely sensed data and the NOAA tide predictions for high tide. We will continue to develop and test our techniques for estimating water elevation from remotely sensed data.

In our efforts to characterize tidal hydrology at our salt marsh sites, there are two primary complications that we are attempting to address.

1. Our DEM products constitute a surface model that often measures the height of vegetation in a region in the salt marsh, not necessarily the peat surface; and,
2. Regions of tall vegetation such as tall form *Spartina alterniflora* or *Phragmites* obstruct the view of water that may be inundating the peat at the base of plant, and so mapping the extent of the water can be difficult.

We are investigating techniques to address these issues, such as adjusting the DEM elevation model by subtracting a central estimate for vegetation height that varies by land cover class, as well as refining

the spectral range or characteristics that indicate regions of inundated peat. Another means at assessing inundation is to adjust the automatic classification algorithm to provide estimates of probability of inundation based on the spectral response and training data.

Automatic Land Cover Classification

In order to characterize land cover and identify threats and vulnerabilities in salt marshes using remote sensing data, we began by linking our multispectral UAS imagery to our *in-situ* field and validation data. We did this through the machine learning algorithm, Random Forests (RF) classifier. Machine learning techniques are well suited for remotely sensed data and linking them to spectrally complex features, such as wetland cover classes, because of their ability to accept nonparametric data and parse through datasets with high-dimensional feature space (i.e. many multispectral bands or many land cover classes). RF, in particular, is a decision tree ensemble classifier that uses many different decision trees, taking the majority 'vote' of all trees to classify a single feature, which is, in this case, a single pixel.

Ground-based field data were used to train and validate the RF classification models. While field crews were not able to collect spatially-balanced classification training data across entire study sites, by using belt transects instead of individual point locations, we were able to provide the classification models with substantial numbers of training pixels, enhancing the potential for high accuracy of the resulting classification.

Different land cover features require different multi-spectral features as model inputs. For example, to map vegetation subclasses, only low tide imagery was used in RF modeling because high tide imagery can occlude vegetation spectral reflectance through inundation. Conversely, to predict bare ground and water classes, high-tide imagery is used.

When run, RF classification outputs several model features. The first is a predicted classification of each pixel in the study site for the given salt marsh classification category of choice; for example, when running models to predict subclasses, each pixel is assigned a single subclass. These predictions can then be turned into categorical classification maps of salt marsh cover types across every study site (Figure 23).

The second model feature is an agreement assessment. Agreement between RF and the salt marsh classification class and subclass categories reference dataset acts as our estimate of model performance. For each classification, training and testing data were randomly split from our ground-truth data and a three-fold cross-validation (CV) methodology was used where either 70% or 60% of the reference polygons were used for training and either 30% or 40% of reference polygons were allocated for testing/validation. Agreement scores can vary considerably based on the assessment metric used. We chose out-of-bag (OOB) and overall agreement to consider more than one line of accuracy assessment. Agreement assessment is reported as percent accuracy at the end of each model run.

A third model feature is the band importance score. This output yields insight into which model input feature (i.e., which multispectral band in a given orthomosaic) was the most 'useful' in classification. This helped us refine which orthomosaics worked best to predict different elements of our Salt Marsh Classification.

The result of RF classification modeling was pixel-based maps showing Salt Marsh Classification features for each of the study sites (Figure 23). For any given map, we also have information on how accurate the

map is and which multispectral information was most important in creating the map. Classification accuracy is an ongoing continuous improvement effort. In some cases, more training data are required to classify and map rare classification features, such as cryptic/sparse vegetation types. As these input data are refined, so is classification accuracy. That said, our consideration of model inputs has yielded land cover classifications across study sites with accuracies that rarely fall below 90.0%.

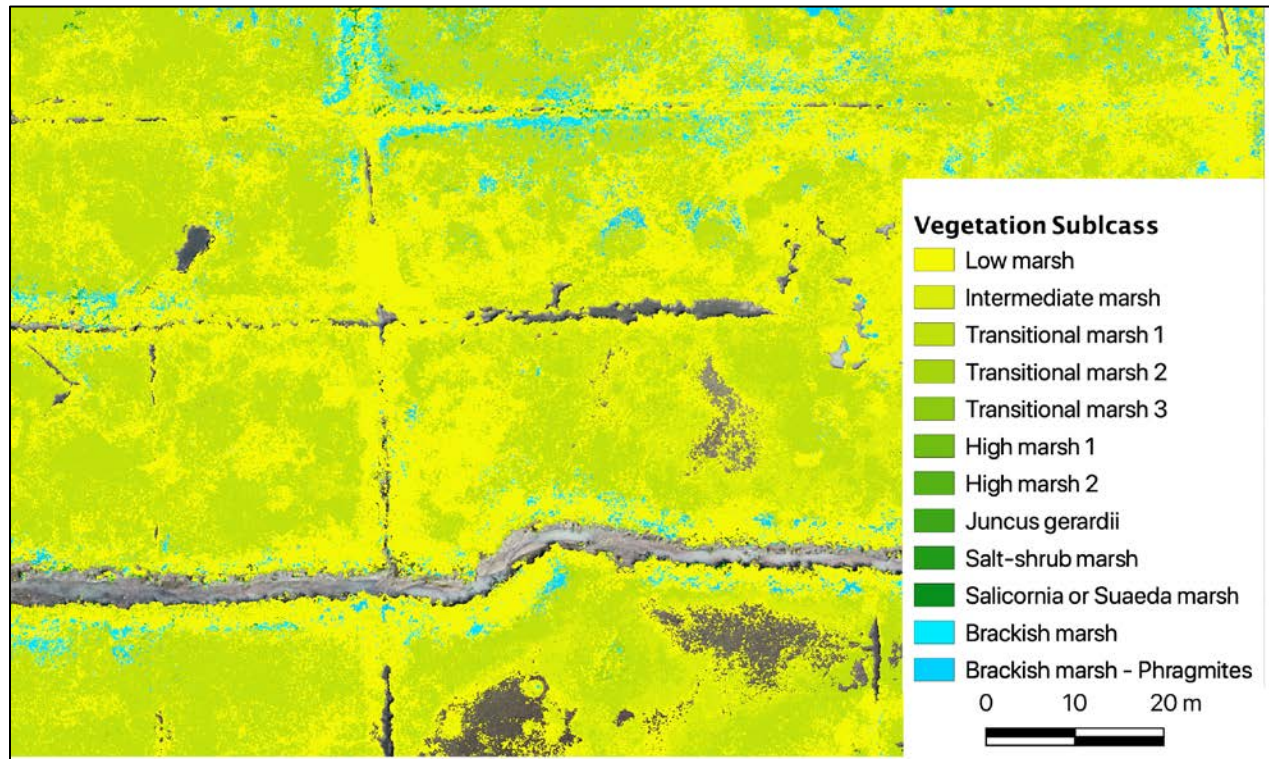


Figure 23. Random Forests land cover classification map of salt marsh vegetation subclasses in our Red River study site.

We have made several study site visits to inspect the spatial and categorical accuracy of our classification maps. Importantly, our models were able to accurately map fine-scale salt marsh features, distinguishing very small patches of bare ground and water classes within a matrix of vegetation (Figure 24). Post-classification field visits to qualitatively assess map accuracy, increased confidence in our results.

The results of automatic classification efforts are (and will be) class and subclass classification maps for every salt marsh study site across Massachusetts.

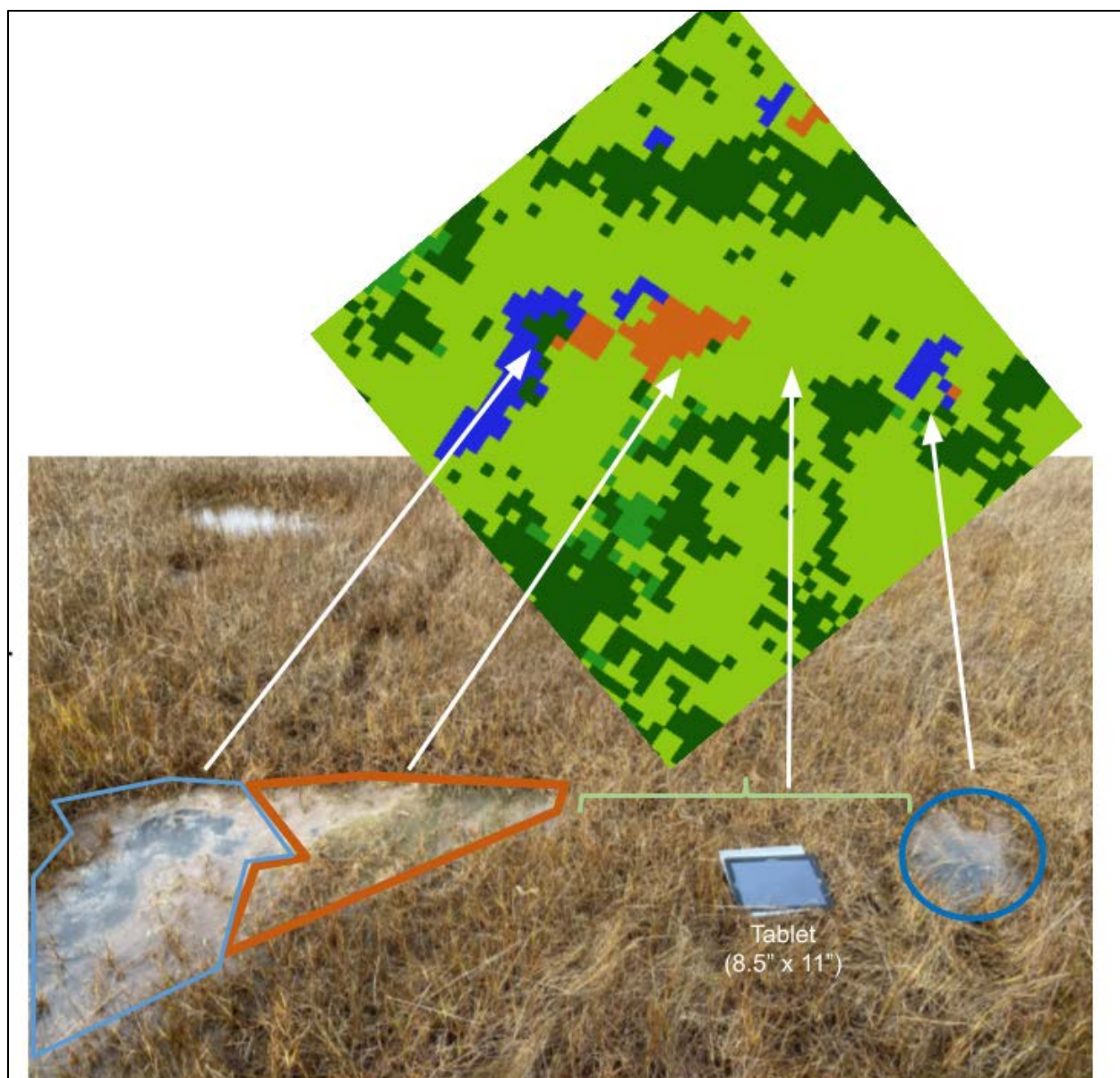


Figure 24: Visual assessment of modeled land cover classification accuracy; shows how the model is able to accurately predict fine-scale salt marsh features such as small pools of water and patches of bare ground within a matrix of dense vegetation.

Probability of Inundation

When running machine learning classification algorithms on spatial data sets, outputs can include both hard and soft (fuzzy) classification. Automatic land cover classification falls under the category of hard classification because a single model feature (a single pixel) can only belong to one classification type. For example, RF hard classification will not allow a pixel to be classified as both water and bare ground at the same time. While this is very useful for creating classification maps, there is no flexibility. However, one benefit of the RF classifier is a 'probability' model output for a given classification. This means for every classification, there is a probability score assigned to each pixel for each class or

subclass, representing the likelihood that the pixel belongs to a given cover class. This allows for much greater flexibility in classification. This type of classification is especially powerful in wetland ecosystems where their inherent land cover classification means they can exist as both water and vegetation simultaneously.

Fuzzy classification has the potential to greatly expand our understanding of salt marsh wetland dynamics and we've employed it in several ways thus far. One of the most powerful applications of our RF fuzzy classification has been a 'probability of inundation' map for each study site. This is derived by running a model to predict salt marsh classes (vegetation, bare ground, and water) and creating a fuzzy classification map of water probability. In this map, every pixel is assigned a likelihood of being water (this can include a probability of 0%), which can be interpreted as the probability of inundation for each pixel. We have run this classification on both low and high tides and are able to compare the difference between the two for insight into hydrological dynamics on the marsh platform. We can even use this to compare the probability of inundation over time to see how different locations on the marsh may be increasing in their inundation probability, potentially representing places that are vulnerable to drowning and die back.

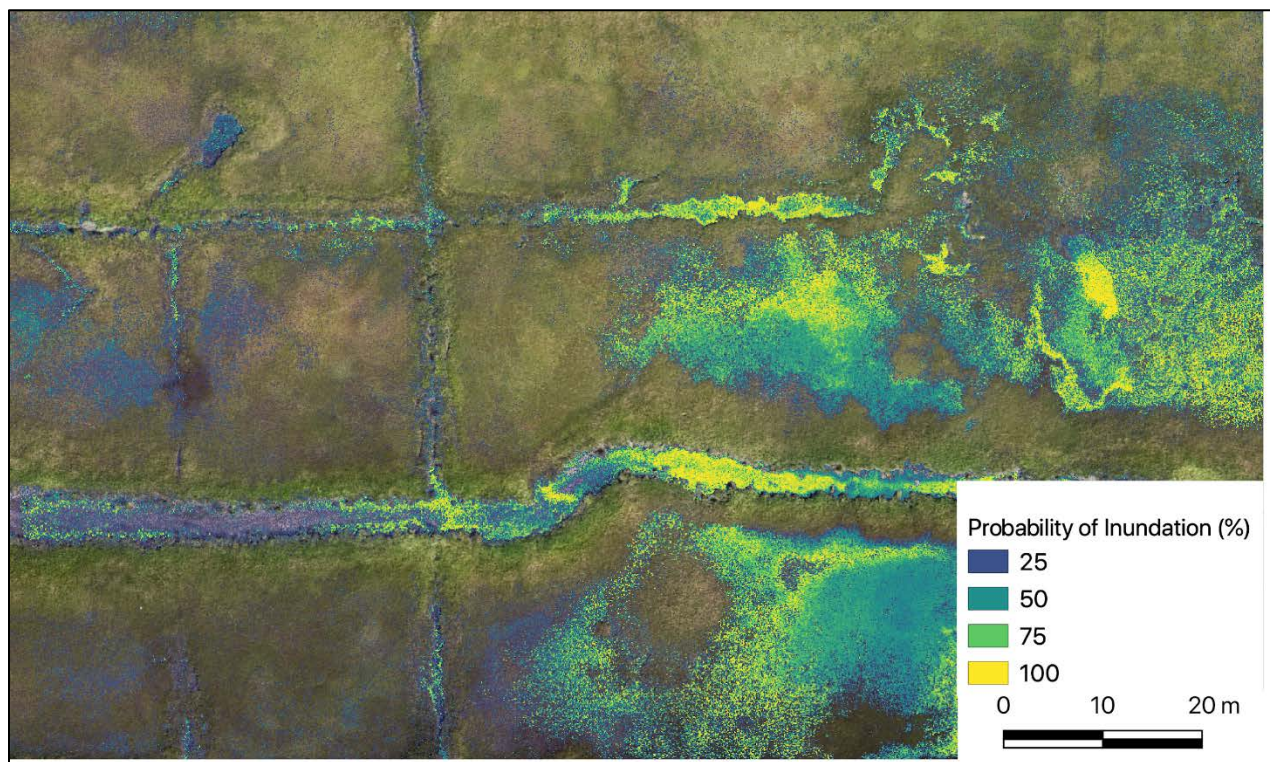


Figure 25. Map of the per-pixel probability of inundation in our Red River salt marsh study site, showing probabilities >25%.

Probability of Subclasses

Similar to running classification on salt marsh classes to map probability of inundation, we are able to run fuzzy classification on salt marsh subclasses. These outputs show the probability of each pixel belonging to a given subclass. For example, we can map the likelihood of *Spartina alterniflora* on the marsh platform (Figure 26). One interpretation of this map is the display of the potential density of *Spartina alterniflora* for any given pixel; this is useful to know because while some pixels may represent pure *Spartina alterniflora* (showing very high probability scores), other pixels may be a dynamic mix of this species with other plants.

In addition to being able to show species cover class ‘mixtures’, we can use these subclass probabilities to explore how hydrological dynamics may interact with different subclasses. For example, we are in the early stages of regression analysis to determine whether different vegetation characteristics may be predictors for marsh vulnerability to increasing inundation due to sea level rise.

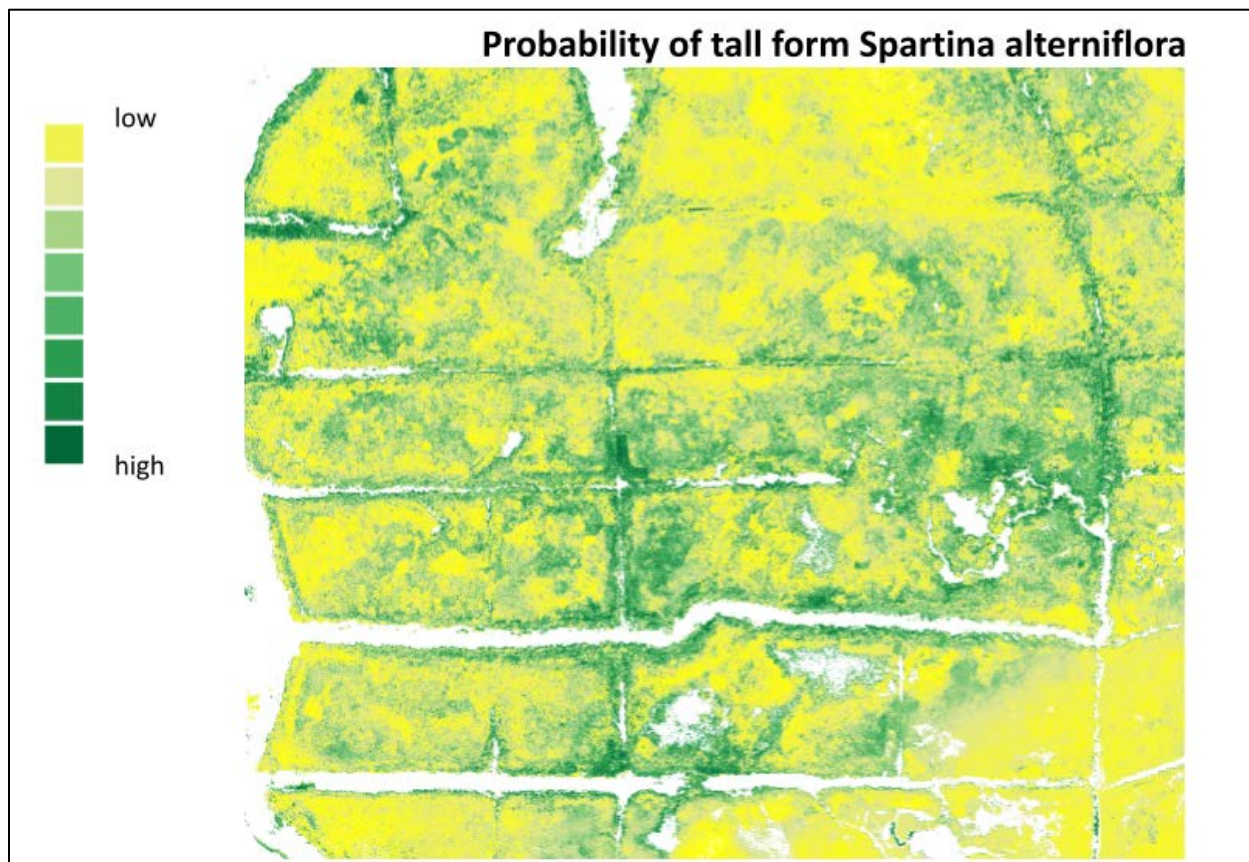


Figure 26. Map of the per-pixel probability of *Spartina alterniflora* vegetation subclasses in our Red River salt marsh study site, showing all probabilities on a relative gradient.

DISCUSSION

The above results took substantial work to produce. Since we started this project, we've had to develop and refine methodologies for field transect inventories, GCP placement, various UAS-related procedures, image processing (photogrammetry and DEM production), field transect to polygon conversion, and various aspects of image-based analysis. In the latter, the processing of temporal stacks of UAS imagery required significant computer processing resources. However, after all this effort to in some ways invent methodology, the various results we demonstrate in various figures above, show both significant progress and promise. We've learned a great deal, and we're producing products that will be extremely useful for analysis of salt marsh change. In this section, we reflect on these lessons learned and challenges we have encountered.

LIMITATIONS / LESSONS LEARNED / CHALLENGES AND CREATIVE SOLUTIONS

Modified Classification

We added new subclasses and attributes to our classification scheme every season after encountering a few areas that could not be accurately represented by the original classification scheme.

Difficulty Accessing Marshes with Large Equipment

While there are many salt marsh environments throughout coastal Massachusetts, not all were suitable for this project. The Great Marsh Wildlife Sanctuary in Barnstable was a desirable site for this project because it is a protected area, is expansive, and is a MA CZM sentinel site; however, it is not easily accessible with large equipment. In order to conduct a UAS flight, the pilot and crew need a staging area during high tide that also provides a clear line of sight on the flying UAV at all times. Accessing a proper staging area at Barnstable was not possible with the larger Matrice 600 UAV but was possible with the smaller Phantom 4 UAV.

Eastern Equine Encephalitis (EEE)

Data collection was temporarily halted in 2019 because of an Eastern Equine Encephalitis (EEE) virus outbreak in Massachusetts. The EEE virus is transmitted to humans by mosquitoes. Mosquitoes were present at all of our sites. Symptoms of EEE are brain swelling, fever, permanent neurological disabilities, and death. While EEE is a very rare disease, 35 communities in Massachusetts were ranked as 'critical risk' and 53 were ranked as "high risk" in late summer 2019. Some salt marsh sites were in communities ranked as "moderate risk" and bordered communities ranked as "high risk". Field data collection and flights were suspended for a brief period of time to protect our team members while community risks escalated. When field data collection resumed, protocols were adjusted to ensure all team members were wearing apparel that protects them from mosquito bites (long sleeves, gloves, head nets, etc.) and had access to mosquito repellent.

Overheated Equipment

Another environmental condition that occasionally stalled the progress of this project was heat, particularly in the mid-to-late summer. All essential field equipment (UAVs and accessories, cell phones, RTK, etc.) exhibited battery-life and connectivity issues when temperatures exceeded 90°F. A canopy tent provided some shade and relief for UAS equipment.

Malfunctioning Equipment

Essential UAS equipment tended to malfunction throughout each season. Returning and repairing UAS equipment was costly and time-intensive. We received malfunctioning equipment from distributors that had to be returned (e.g. a MicaSense RedEdge sensor), experienced months-long delays with a UAS repair service, and waited for foreign-made parts needed for routine maintenance and repairs. Delays were offset by having several back-up UAVs available for flights while our main UAV (Matrice 600) was being serviced. Although the back-up UAVs could not carry both a MicaSense RedEdge and SWIR sensors in tandem like the Matrice 600, we were able to mount a MicaSense RedEdge to the Matrice 210 and use a Phantom 4 to gather RGB and elevation data to build DEMs.

Tagging GCPs

An important first step in creating accurately aligned orthomosaics in AgiSoft was validating the x, y, and z (elevation) coordinates of each GCP. While these measurements were taken accurately in the field, they had to be matched with UAS images containing the GCPs. Image processing personnel had to validate the position of each GCP (a process called “tagging”) in each separate image that captured the GCP, in each spectral band. This was a time-intensive endeavor that required 6-8 hours of additional staff time for a single day’s worth of flights (three flights) that used the MicaSense RedEdge and SWIR sensors.

Access to Sufficient Computer Processing Capacity

When we started the project we built two high end remote desktops to do our Agisoft photogrammetry processing and our remote sensing image analysis work. Once we reached the point that we had enough orthomosaic imagery for a particular site, we quickly realized these high end desktop computers were not sufficiently powerful to meet the massive computational requirements needed for the land cover classification and other analyses. Consequently, in year 2019-20, we gained access to the Holyoke High Performance Computer Cluster – a supercomputer we call “Unity.” After some months learning how to operate high end remote sensing techniques on this platform, we had much improved computational performance. Functions that that would take days or even weeks to complete on the high end remote desktops, could be performed in minutes on Unity. This was a vast improvement in the speed of our computational analyses. In addition, we wrote processing scripts in Python that allowed us to run the same workflows for other sites using the same custom analytical software. These were all important successes and advances for this study. However, these advances were not without their own hurdles. We share the Unity supercomputer with other research efforts, and this platform requires periods of maintenance and does, on occasion, crash when asked to execute processes like orthomosaic alignments. All-in-all however, these computational challenges and our solutions represent important advances for this project.

COVID-19

Travel restrictions, infected personnel, isolation and quarantine periods, and changes in university research and hiring policies during the COVID-19 pandemic, contributed to delays in our 2020 field season. We also were not able to incorporate any new salt marsh sites into our portfolio due to COVID-19 concerns. We developed new COVID-19 research protocols and eventually received approval from the University to resume data collection later in the 2020 field season.

NEXT STEPS

We are continuing to optimize classification models for all sites. In early spring 2021, before vegetation emerged, we flew each site at low tide with a Phantom 4 Pro camera in order to build a DEM that better approximates a Digital Terrain Model (DTM) for each site. By capturing a marsh before it “greens up”, we expect the DEM or DTM produced will more accurately reflect the substrate topography rather than vegetation height, and elevation errors will be greatly reduced. We expect that these improved DTMs will strengthen hydrology-related classification models and allow us to better identify areas of erosion.

As automatic classification outputs are generated for each site, we anticipate a need to revisit the sites with a Trimble RTK and validate/correct data products, correct additional training/validation data, and improve the accuracy of our classification scheme.

As progress in understanding salt marsh vegetation and hydrology dynamics as seen through multispectral UAS imagery continues, so does our understanding of how to guide future machine learning classification models. We anticipate a mixture of hard classifiers and fuzzy classifiers to emerge as unique metrics of marsh vulnerability and integrity for different research questions (Table 6).

Table 6 - Examples of research questions about marsh health and the machine learning classification products.

Classification Product	Research Question Example
Hard classifier of classes (Water, Bare Ground, Vegetation)	Where on the marsh is there water or bare ground in areas where they aren’t expected? (identifying marsh dieback, submergence)
Fuzzy classification of classes (Water, Bare Ground, Vegetation)	What is the probability of inundation across the marsh? (vulnerability to submergence)
Hard classifier of vegetation subclasses (i.e. species level identification)	Where do vegetation subclasses that indicate poor marsh health occur on the marsh? (vulnerability to submergence, dieback or other stressors)
Fuzzy classifier of all subclasses	Where do high probabilities of high marsh vegetation and high probabilities of inundation co-occur? (tendency toward submergence)

In addition to ongoing progress on pixel-based spectral analysis of UAS imagery, we have begun to add a conceptual model for object-oriented analysis of geomorphological features on the marsh. This includes identifying marsh features and phenomena such as bank slumping, widening creek channels, and other types of erosion. This type of work is distinctly different from pixel-based spectral analysis because it

considers a cluster of pixels together (considered a “feature”). We plan on working with the UMass Amherst Center for Data Science to utilize cutting edge computer-vision methodologies to help answer key research questions about marsh features.

CONCLUSIONS

The purpose of this project is to determine whether a combination of remote sensing technology, ground truthing, and machine-based learning can help scientists and stakeholders map, monitor, and assess salt marsh ecosystems. In this phase of the project we created and tested detailed protocols in preparation for salt marsh data collection, collected an extensive amount of spectral data from salt marshes using remote sensing technology, collected a substantial amount of on-the-ground data for use in model training and validation, and have begun analyzing data using complex modeling approaches. We can confirm that spectral data collected with UAS coupled with on the ground data collection and machine-based learning, can accurately classify salt marsh landscapes at a finer resolution than other approaches currently in use.

CONTACT INFORMATION

Scott Jackson, Extension Professor
Department of Environmental Conservation
Holdsworth Hall
University of Massachusetts
Amherst, MA 01003
(413) 545-4743
sjackson@umass.edu